DURABILITY OF FIBRE REINFORCED POLYMER [FRP] COMPOSITE PIPE

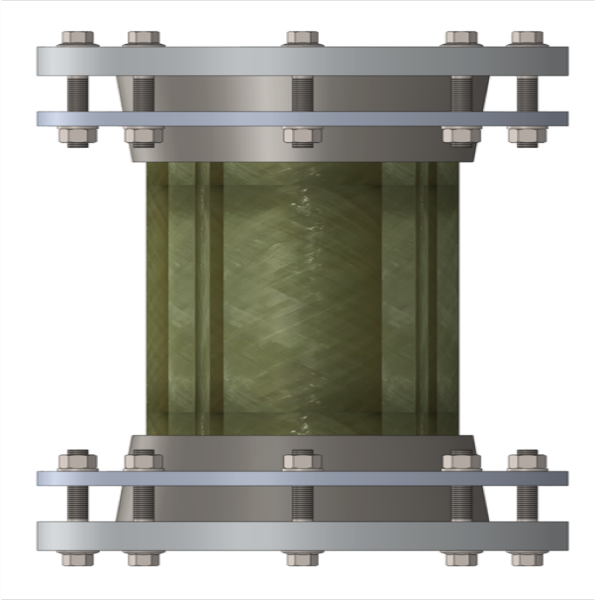

Presented by : Francisco Xavier Ximenes

This Thesis is Proposed to Obtain the Master Engineering Degree in Mechanical Engineering of Faculty of Engineering, University of Porto

Supervisor : Prof. António Torres Marques, Ph. D

FEUP

2017
Mechanical Engineering
Faculty of Engineering
University of Porto

Motto;

Our biggest challenge is developing man power and human resource; without it we can't develop country in other areas.

General, Taur Matan Ruak
President of The Republic Democrat of Timor Leste
(2012-2017)

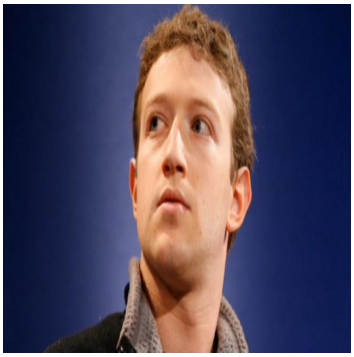

Give everyone the power to share anything with anyone.

Mark Zuckerberg
Facebook Founder

Thank you for

My parents, they always support by their suggestions in God and to give me energy to overcome many challenges from my whole study.

Acknowledgements

My great honor to Prof. Antonio Torres Marques, Ph D. for his guidance as thesis supervisor for the time being of this work.

Specials thank to Prof. Rui Miranda Guedes Ph. D for his guidance from the part of failure time analysis of composite materials and Prof, Miguel A. V. de Figueiredo, Ph. D and Hugo Faria, Ph D. for laboratory, experimental guidance.
Many thanks to Mechanical Engineering Department, Faculty of Engineering, University of Porto and INEGI-UPorto, specially to Composite Materials Testing Laboratory Team and Machining Centre Team from the design and production of FRP HFW composite pipes and laboratory experiments for their warm cooperation and suggestions that had very valuable for me until finished my experimental modelling and data acquisition.

Finally, many thanks to Mechanical Engineering Department of Faculty of Engineering, Science and Technology, National University of Timor Leste for their support for funding my whole study in University of Porto by the capacity development of human resource development fund under the Ministry of Education, The Government of Republic Democrat of Timor Leste.

Abstract

Fibre reinforced polymers, like FRP composite pipes, nowadays, become attractive solutions in many industries. Therefore, FRP composite pipes helicoidal filament winding, HFW, are considered as priority for many researchers to develop the excellent/optimal properties for industry applications. The helicoidal filament winding, HFW, production for FRP structures is made with different fibre directions HFW$\pm$45˚ and HFW$\pm$55˚ passing by an unsaturated polyester resin bath. Tests will be performed in different ageing conditions for different temperatures regarding industrial applications. Properties phenomena in burst pressure of FRP composite pipes test, tensile test with samples from FRP composite pipes and three-point bending creep test with samples from FRP composite pipes explore the FRP composite pipes performance in offshore and onshore industries, high pressure pipelines, and aircraft industries.

For different ageing properties; unconditioned, water immersion, WI, sea water immersion, SWI, diesel immersion, DI, at ambient temperature and water immersion, WI, at 60°C of FRP HFW composite pipes, the viscoelastic and viscoplastic of FRP HFW for different stress level configuration 1%, 1,4%, and 1,8% have shown reduction of the deflection rate of three-point bending creep test and becomes the evaluating data properties of FRP HFW to the failure time analysis. The failure lifetime of FRP HFW composite pipes correspond to the industry applications.

Keywords

Filament winding, composite pipes, fibre directions, unsaturated polyester resin, ageing, burst pressure test, three-point bending creep test and failure lifetime analysis.

Table of Contents

List of Tables

List of Figure

List of Abbreviations

API	American Petroleum Industry
AWWA	American Water Works Association
ASTM	American Society of Testing and Materials
CATMAN 4,5	Software for three-point bending data analysis
CC-FRP	Centrifugal Casting of Fibre Reinforced Polymers
CFW	Continuous filament winding
CEN	European Committee for Standardization
DI specimen	Diesel Immerse specimen
3PBT Machine	Three-Point Bending Machine
FRP	Fibre Reinforced Polymers
HFW $\pm 45^{\circ}$	Helicoidal Filament Winding $\pm 45^{\circ}$
HFW $\pm 55^{\circ}$	Helicoidal Filament Winding $\pm 55^{\circ}$
GRP System	Glass Reinforced Polymers System
HDB	Hydrostatic Design Basis
ISO	International Standard Organization
LVDT	Linear Variable Displacement Transducer
PDB	Pressure Design Basis
SWI specimen	Sea Water Immerse specimen
U specimen	Unconditioned specimen
WI specimen	Water Immerse specimen
P1U45TT	U Specimen HFW $\pm 45^{\circ}$ of FRP composite pipes for Tensile Test at ambient temperature
P3U45TT	U Specimen HFW $\pm 45^{\circ}$ of FRP composite pipes for Tensile Test at ambient temperature
P4U45TT	U Specimen HFW $\pm 45^{\circ}$ of FRP composite pipes for Tensile Test at ambient temperature
P7D45TT	DI specimen HFW $\pm 45^{\circ}$ of FRP composite pipes for Tensile Test at ambient temperature
P6SWI45TT	SWI specimen HFW $\pm 45^{\circ}$ of FRP composite pipes for Tensile Test at ambient temperature
P12W45TT	WI specimen HFW $\pm 45^{\circ}$ of FRP composite pipes for Tensile Test at ambient temperature
P9W45TT-T60	WI specimen HFW $\pm 45^{\circ}$ of FRP composite pipes for Tensile Test at $60^{\circ}C$
P15W45TT-T60	WI specimen HFW $\pm 45^{\circ}$ of FRP composite pipes for Tensile Test at $60^{\circ}C$
P1U55TT	U specimen HFW $\pm 55^{\circ}$ of FRP composite pipes for Tensile Test at ambient temperature

P15U55TT	U specimen HFW ±55° of FRP composite pipes for Tensile Test at ambient temperature
P16U55TT	U specimen HFW ±55° of FRP composite pipes for Tensile Test at ambient temperature
P3D55TT	DI specimen HFW ±55° of FRP composite pipes for Tensile Test at ambient temperature
P5W55TT	WI specimen HFW ±55° of FRP composite pipes for Tensile Test at ambient temperature
P8SWI55TT	SWI specimen HFW ±55° of FRP composite pipes for Tensile Test at ambient temperature
P6W55TT-T60	WI specimen HFW ±55° of FRP composite pipes for Tensile Test at 60°C
P5U453PBT	U specimen HFW ±45° of FRP composite pipes for three-point bending creep test at ambient temperature
P10SWI453PBT	SWI specimen HFW ±45° of FRP composite pipes for three-point bending creep test at ambient temperature
P13D453PBT	DI specimen HFW ±45° of FRP composite pipes for three-point bending creep test at ambient temperature
P8W453PBT	WI specimen HFW ±45° of FRP composite pipes for three-point bending creep test at ambient temperature
P11W453PBT-T60	WI specimen HFW ±45° of FRP composite pipes for three-point bending creep test at 60°C.
P14U553PBT	U specimen HFW ±55° of FRP composite pipes for three-point bending creep test at ambient temperature
P4SWI553PBT	SWI specimen HFW ±45° of FRP composite pipes for three-point bending creep test at ambient temperature
P10SWI553PBT	SWI specimen HFW ±45° of FRP composite pipes for three-point bending creep test at ambient temperature
P10SWI553PBT	SWI specimen HFW ±45° of FRP composite pipes for three-point bending creep test at ambient temperature
P7D553PBT	DI specimen HFW ±45° of FRP composite pipes for three-point bending creep test at ambient temperature
P13W553PBT	WI specimen HFW ±45° of FRP composite pipes for three-point bending creep test at ambient temperature
P7W553PBT-T60	WI specimen HFW ±45° of FRP composite pipes for three-point bending creep test at 60°C.

List of Symbols

$A_{\phi,\theta}$	Area of the FRP tubular composite pipes HFW $\pm 45^{\circ}$ and HFW $\pm 55^{\circ}$ [mm^2]
$A_{\phi,\theta}$	Area of the FRP composite pipes beam tensile test of HFW $\pm 45^{\circ}$ and HFW $\pm 55^{\circ}$ [mm^2]
a	Intercept of the strain failure time axis burst pressure [-]
b	Circular arc beam length [mm]
b	Slope of the line of burst pressure test [-]
$b_{\phi,\theta}$	Circular arc beam length of the FRP composite pipe HFW $\pm 45^{\circ}$ and HFW $\pm 55^{\circ}$ [mm]
$b_{1_{\phi,\theta}}$	Intercept of failure time at three-point bending creep test [-]
$b_{2_{\phi,\theta}}$	Slope of failure time at three-point bending creep test [-]
$D(t)$	Three-point bending machine displacement [mm]
$D_{\phi,\theta}(t)$	Creep displacement of the FRP composite pipes HFW $\pm 45^{\circ}$ and HFW $\pm 55^{\circ}$ [mm]
$D_{\phi,\theta}$	Diameter of FRP composite thin pipe HFW $\pm 45^{\circ}$ and HFW $\pm 55^{\circ}$ [mm]
$d(y)$	Deflection of three-point bending specimen [mm]
$\varepsilon_{\phi,\theta}$	Creep strain of three-point bending creep test [-]
$\varepsilon_{f_{\phi,\theta}}$	Variable of strain of FRP composite pipe failure time [-]
$\varepsilon_{Max_{\phi,\theta}}$	Maximum tensile strain [-]
$\log\left(\varepsilon_{f_{\phi,\theta}}\right)$	Strain at failure time three-point bending creep test [-]
F	Force [N]
$F_{\phi,\theta}$	Tensile force of HFW $\pm 45^{\circ}$ and HFW $\pm 55^{\circ}$ FRP composite pipes [N]
$F_{Max_{\phi,\theta}}$	Force level configuration of circular arc beam HFW $\pm 45^{\circ}$ and HFW $\pm 55^{\circ}$ FRP composite pipes [N]
I	The inertia of circular beam of FRP composite pipes of the FRP composite pipes HFW $\pm 45^{\circ}$ and HFW $\pm 55^{\circ}$ [mm^4]
$J_{\phi,\theta}(t)$	Creep compliance of three-point bending creep test [1/MPa]
L_1	Length of FRP composite thin pipe burst pressure test [mm]
L_1	Length of FRP composite pipe circular arc beam tensile test and three-point bending creep test [mm]
M	Bending moment [Nm]
P	Internal pressure of FRP composite thin pipe [N]
r	Radius of circular arc beam tension test [mm]
r	Radius of circular arc beam three-point bending creep test [mm]
r	Radius of FRP composite pipe tube [mm]
$t_{\phi,\theta}$	Thickness of FRP composite pipes HFW $\pm 45^{\circ}$ and HFW $\pm 55^{\circ}$ [mm]

$t_{u_{\phi,\theta}}$	Variable of time dependent HFW $\pm 45^{\circ}$ and HFW $\pm 55^{\circ}$ of FRP composite pipe [minutes]
$\log(t_u)$	Time to failure in three-point bending creep test [minutes]
y	Distance at center of circular arc beam [mm]
$\sigma_{C_{\phi,\theta}}$	Circumferential stress of FRP composite thin pipe HFW $\pm 45^{\circ}$ and HFW $\pm 55^{\circ}$ [MPa]
$\sigma_{L_{\phi,\theta}}$	Longitudinal stress of FRP composite thin pipe HFW $\pm 45^{\circ}$ and HFW $\pm 55^{\circ}$ [MPa]
σ_{Max}	Maximum tensile stress [MPa]
$\sigma_{Max_{\phi,\theta}}$	Maximum tensile stress of FRP composite thin pipe HFW $\pm 45^{\circ}$ and HFW $\pm 55^{\circ}$ [MPa]
β	Semicircular angle of FRP composite pipes circular arc beam
ϕ	Helicoidal Winding $\pm 45^{\circ}$
θ	Helicoidal Winding $\pm 55^{\circ}$
θ	Circular arc beam angle

1. Introduction

1.1 Fibre Reinforced Polymers (FRP) Composite Pipes

Ageing of fibre reinforced plastic (FRP) composite pipes have been discussed during several decades for attractive applications [1]. Particularly, FRP proved in many unique properties, such as: lightweight, high stiffness, corrosion resistance, abrasion resistance and tailor ability to various configurations of FRP composite pipes usable for more than 50 years [2]. The FRP composite pipes have been used in the chemical industry and its products, offshore facilities, transportation systems and sewage systems.

Nowadays, researchers and pipe industries consider that FRP composite pipes durability for short and long term applications are very trustworthy for high risk conditions. However, many challenges in these studies are still ongoing for many combinations in environmental issues, stress and strain analysis, viscoelastic behavior, failure analysis and lifetime prediction [3].

In this study, overall modeling, by analytical formulation and experimental study, to define the existing effects on FRP composite pipes from different type of construction namely helicoidal filament winding (HFW), centrifugal casting and hybrid ones that has been developed. The comparisons with European Committee for Standardization [CEN], International Organization Standard [ISO], American Water Works Association [AWWA] and American Petroleum Institute [API] are presented.

1.2 Background and Motivation

Overall market for FRP composite pipes is growing 14% [4], estimated from the size of the world composite market. Many industries start changing the traditional pipes to FRP composite pipes system. Even FRP composite pipes materials have relative high cost ratio to the installation and maintenance cost. Generally, FRP composite pipes materials offer many advantages for structural design of oil rigs, offshore and onshore power plant, aircraft fuselage, helicopter rotor shaft, high pressure pipelines, military landing craft and sport goods [1-12, 21-40].

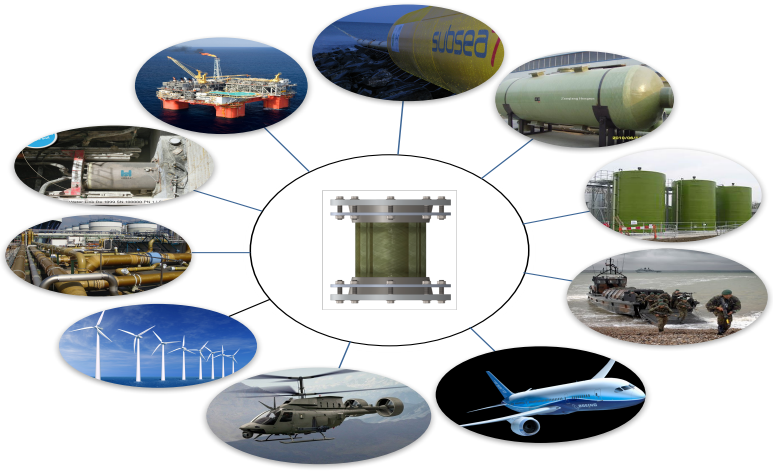

Figure 1. FRP composite applications

There are varieties of fibre composite materials which are normally graded and manufactured based on the applications and not definite types or classes of composite materials. The FRP composite pipes materials that are commercial available use glass fibres or carbon fibres combined with resins.

FRP composite pipes are considered, most substantially, in offshore applications for oilfield mining operation such as drilling [5], logging, completion, production and workover, depth sea pipelines, onshore pipelines, tanks, storages vessels, injection liner and structures. More advantages of FRP composite pipes are of extremely importance in high acidic and corrosive environment, non-conductive and non-magnetic, and high-temperature polymer composites are considered being ideal materials for construction types [1,5,6].

Several pipeline explosions and spills in the oil industries have come to the forefront of the researcher's attention in recent years. Industries active in the repair of pipeline [7] estimate that there is a potential market of over 200,000 km of pipelines that will be required by ultra-deep water applications targeting beyond 4000 meters' depth at 60˚C [1-10,21-40].

The main goal of this research is to investigate the durability of FRP composite pipes w.r.t. the influence of environmental effects (humidity, temperature and acidic), helicoidal filament winding effects, centrifugal casting, creep test, structural characteristic of FRP composite pipes, internal pressure, handling of FRP composite pipes properties, three-point bending properties and failure analysis evaluation [1-10, 12, 21-40].

1.3 Research Methodology

Basically, this thesis is based on analytical formulation and experimental study to solve the problems identified on FRP composite pipes design. Evaluation and life prediction of FRP composite pipes in moisture and having thermal effects, with productions helicoidal

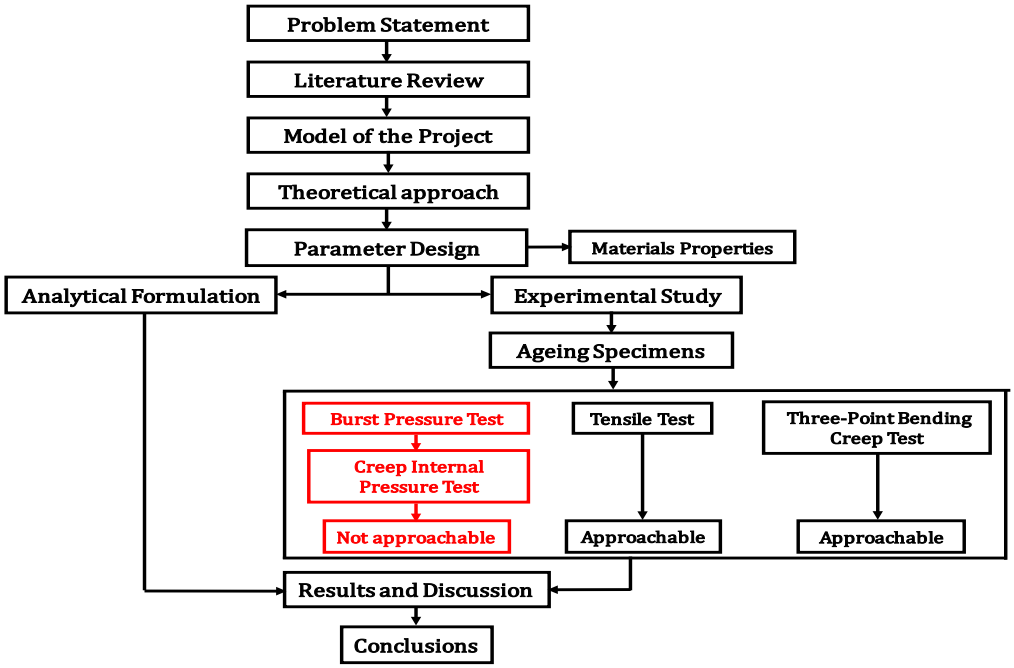

Figure 2. Research methodology

filament winding, HFW, processes and structural complexity of FRP composite pipes analysis, are identified to perform optimum properties.

1.4 Thesis Layout

This thesis is divided in five sections. The first chapter is introduction, second chapter is literature review, third chapter is theoretical analysis and experimental study, fourth chapter is results and discussion, and chapter five presents the conclusions. To summarize all topics could be explained in general, the first introduces briefly the advantage of FRP pipes unique properties, such as high stiffness, corrosion resistance and abrasion resistance of FRP composite pipes usable more than 50 years. The second chapter deals with literature review consisting of general application of FRP composite pipes, temperature condition of FRP composite pipes, short-term behavior of FRP composite pipes, FRP composite pipes standard and failure analysis of FRP composite pipes.

The third chapter is theoretical analysis and experimental study that includes the short-term test of burst pressure, tensile strength, short term test for creep internal pressure, creep three-point bending strength. Experimental study is referred to burst test of helicoidal filament winding, HFW, tensile test, creep internal pressure test, three-point bending creep test structural characteristic of FRP composite pipes. The fourth chapter is results and discussion, consisting of the analytical formulation and experimental study of FRP composite pipes. The fifth chapter is conclusions to summarize the results and discussion from the experimental study and theoretical analysis formulation [18, 19, 24].

1.5 References

1]. Kim H-Y, Y-H. Park, Y-J, You and C-K, Moon (2008)."Short-term durability test for GFRP rods under various environmental conditions." Composite Structures 83(1):37-47.

2]. Krishnan P, M. S. Abdul Majid, M. Afendi, A. G. Gibson and H. F. A. Marzuki (2015). "Effects of winding angle on the behaviour of glass/epoxy pipes under multiaxial cyclic loading." Materials & Design 88: 196-206.

3]. Rafiee R. (2016) On the mechanical performance of glass-fibre-reinforced thermosetting-resin pipes: A review. *Elsevier Ltd*, 143, 151-164.

4]. Composites, J. M. (2015, May-June). *The USA believe in Composites*. Retrieved from www.JECcomposites.com.

5]. Eslami S. (May, 2013). *Durability of Perforated GFRP under various environmental conditions with emphasis on its application as a liner for directional oil wells.* Halifax, Nova Scotia: Ph. D Thesis.

6]. Gibson A. G, Ortheguy Torres M. E, Browne T.N.A, Feih S, and Mouritz A.P, (2010). High temperature and fire behaviour of continuous glass fibre/polypropylene laminates. *Composite: Part A, 41*, 1219-1231.

7]. Keller Michael W, Jellison B. D. and Ellison T. (2013). Moisture effects on the thermal and creep performance of carbon fiber/epoxy composite for structural pipelines repair. Composite: Part B, *Elsevier Ltd*, 45, 1173-1180.

8]. Moser A. P, (2001). *Buried pipe Design, Second Edition.* McGraw-Hill.

9]. Baker A, Dutton S, and Kelly D, (2004). *Composite Materials for Aircraft Structure* (Second Edition ed.). American Institute of Aeronautics and Astronautics, Inc.

10]. Associates, E. G. (1999). *Marine Composites, Second Edition.* Eric Greene Associates, Inc.

11]. AWWA Manual M45, First Edition. (1999). *Fiberglass Pipe Design.* American Water Works Association .

12]. Guo B, Song S, Ghalambor A, and Lin T, (2014). *Offshore Pipelines (Design, Installation and Mantenance) Second Edition.* Elsevier Inc.

13]. D1598-02, ASTM. (2002). Standard Test Method for Time-to-Failure of Plastic Pipe Under Constant Internal Pressure.

14]. D1599-99, ASTM. (2000). *Standard Test Method for Resistance to Short-time Hydraulic Pressure of Plastic Pipe, Tubing, and Fitting.* ASTM International.

15]. D2990-01, ASTM. (2001). *Standard Test Method for Tensile, Compressive, and Flexural Creep and Creep-Rupture of Plastics.* ASTM International .

16]. D2992-01, ASTM. (2001). *Standard Practice for Obtaining Hydrostatic or Pressure Design Basis for "Fiberglass" (Glass-Fiber-Reinforced Thermosetting-Resin) Pipe and Fitting.* ASTM International.

17]. D3039/D3039M-00, ASTM. (2000). *Standard Test Method for Tensile Properties of Polymer Matrix Composite Materials.* ASTM International.

18]. D3517-04, ASTM. (2004). *Standard Specification for "Fiberglass" (Glass-Fiber-Reinforced Thermosetting-Resin) Pressure Pipe.* ASTM International.

19]. D638-08, ASTM. (2008). *Standard Test Method for Tensile Properties of Plastics.* ASTM International.

20]. D790-02, ASTM. (2002). *Standard Test Method for Flexural Properties of Unreinforced and Reinforced Plastics Electrical Insulating Materials.* ASTM International.

21]. Dons, K. (June 2013). *Filament winding of composite tubes.* Norway: Norwegian University of Science and Technology, Mechanical Engineering, Master of Science Thesis.
22]. Greentech, G. (2016) "FRP Pressure Pipe". Retrieved from www.gilgwang.co.kr.
23]. Hoa, S. V. (2009). *Principles of the Manufacturing of Composite Materials.* DEStech Publications, Inc.
24]. Hodgkinson, J. M. (2000). *Mechanical testing of advanced fibre composite.* Woodhead publishing limited Cambridge England
25]. Hossain, M. E. (2011). The current and future trends of composite materials: an experimental study. *Journal of Composite Materials*, 2133.
26]. Karpuz, P. (May, 2005). *Mechanical characterization of filament wound composite tubes by internal pressure testing.* Master thesis of Metallurgical and Materials Engineering, Middle East Technical University.
27]. Kleschinski M, Muller D, (Springer. 2005). *Composite Structures for Ocean Energy Applications.* Otto-Hahn-Strabe 5, 34123 Kassel: xperion ALPHA Composites GmbH.
28]. Abdul Majid M. S, Afendi M, Afendi P, M. Haslan, Krishnan P, Amin A. M, (2014). Ageing effects on burst pressure test of impacted glass fibre reinforcement epoxy (GRE) pipes. *Trans Tech Publications, Switzerland, 695*, 717-720.
29]. Mallick P. K, (2007). *Fiber-Reinforced Composite (Materials, Manufacturing, and Design) Third Edition.* Taylor and Francis Group, LLC.
30]. Braestrup M. W, J. B, Andersen L. W, Bryndum M, Christensen C.R, Nielsen N.J.R. (2005). *Design and Installation of Marine Pipelines.* Oxford OX4 2DQ, UK: Blackwell Science Ltd.
31]. Marsh, G. (2009). Composite pipe capture water and sewage markets. *Reinforced Plastics*, 53, 18-21.
32]. Davies P, Boisseau A, Choqueuse D, Peters L, Renaud C, Nickel R, Thiebaud F, Perreux D, (2010). Marine Composite for Ocean Energy Application: Ensuring long-term durability. *Third International Conference on Ocean Energy.*
33]. Pavlov D. G, (2013) Composite Materials in Piping Application: Design, Analysis and Optimization of Subsea and Onshore Pipelines from FRP Composites. DEStech Publication, ISBN No. 978-1-60595-029-7
34]. Dasappa P, L-S. Pearl, Xiao X, (2009). Temperature effects on creep behavior of continuous fiber GMT composites . *Elsevier Ltd, Part A 40*, 1071-1081.
35]. Deolia P, Shaikh F. A, (2016). Burst pressure analysis of a pressure vessel: A review. *International Journal of Research in Advent Technology*, 2321-9637.
36]. Guedes R. M, Sá A, (2007). Influence of moisture absorbtion on creep of GRP composite pipe. *Elsevier Ltd (Polymers Testing)*, 595.
37]. Braskoro S, Dronkers T. D. T, Driel M. van, (2004). From Shallow to Deep Implications for Offshore Pipeline Design. *Indonesian Oil and Gas Community*.
38]. Beckwith S, Greenwood M, (May, 2006). Don't Overlook Composite FRP Pipe. *www.che.com*, 42.
39]. Yoon S. H, Oh J. O, (2015). Prediction of long term performance for GRP pipes under sustained internal pressure. *Composite Structure*, 134, 185-189.
40]. Bai Y, Bai Q, (2012). *Subsea Engineering Handbook.* Elsevier Inc

2. Literature Review

2.1 General Application of FRP Composite Pipes

The multipurpose of FRP composite pipes applications in various industries shows that the advantages of FRP composite pipes are relatively lightweight to transportation cost, have easy and rapid installation [1]. In the harsh condition, FRP composite pipes is still durable, ultraviolet resistant and corrosion resistant therefore maintenance cost is minimal. The applications of FRP composite pipes in chemical industry are used for sugar refineries, resin plants, aluminum production plants, mining (slurries), cooling systems and fire water for industrial facilities and process piping and other industrial manufacturing applications [2-5].

In offshore facilities, FRP composite pipes are showing more durable in marine environments and highly aggressive resistant w.r.t. the traditional steel pipes that have to be replaced two or three times in offshore production such as oil production rigs, high power production (wind turbine) rigs and depth sea pipelines [2-5,11].

For infrastructures in transportation system and sewage system, FRP composite pipes are used for water and sewer pipelines. Considering the internal and external attacks of traditional steel pipes and concrete pipes with effect on ferrous and cementitious materials, FRP composite pipes becomes as the latest advance in technology piping for new infrastructures construction for transportation and sewage system.

2.2 Temperature Condition of FRP Composite Pipes

2.2.1 FRP Composite Pipes and Humidity

FRP composite pipe materials are influenced by environment, i.e. air, natural water, sea water, and soils absorptions. Water absorption tends to slow down reaching saturation after immersion during some periods of time. The properties of FRP composite pipes in moisture absorption changed in thermo-physical, viscoelastic, mechanical and plasticization. Hydrolysis initiates in the polymeric matrix and goes-up to degradation at the extremely temperature [6,7].

In these circumstances, it is necessary to estimate the moisture concentration and the hygrothermal internal stress fields to evaluate the durability for the time dependent applications of FRP composite pipe [8]. In certain cases, the moisture concentration effect combined with temperature and relative-humidity cycles over a period of time, either near the inner or near the outer surface, may cause debonding between fibre and matrix.

2.2.2 Temperature

Unexpected phenomenon on FRP composite pipes can be caused by fire [9], freeze-thaw cycles, elevated and subfreezing temperature and thermal cycles [10,11]. The intense deterioration of the bulk resin and the fibre-matrix interface temperature shall be above the service temperature of FRP composite pipes. In addition, with an increase in viscoelastic response the consequence is the reduction in mechanical performance which can arise particularly, when resins are subjected to an elevated temperature range.

At subzero temperature, however, the FRP composite pipes would harden the matrix with the influence on fibre micro-cracks from load effects and bond degradation of fibre, and matrix reduces stiffness [13]. Furthermore, the combination of freeze-thaw cycles and presence of salt propagation at FRP composite pipe surface can cause formation of salt deposits in size and magnitude and drying may lead to significant degradation.

2.3 FRP Composite Pipe Production Standard and Prediction of Properties Methodology

2.3.1 FRP Composite Pipes Production

The FRP composite pipes analyzed here are produced by three different methods, such as helicoidal filament wound, HFW, and continuous filament winding, CFW, centrifugal casting and hybrid [1,12,14-18]. FRP composite pipes of HFW process use a conventional mandrel rotating and dry fibres passing through a resin bath and winding over the conventional mandrel whilst moving in axial direction. The impregnated fibres are wound around the mandrel with lateral movement in different helicoidal winding and different layers along the conventional mandrel to achieve the desired thickness of the FRP composite pipes.

The final FRP composite pipe is transferred, on mandrel, to the curing station where the curing can be induced by an infrared lamp and maintaining rotation of mandrel or curing in an oven. After the FRP composite pipes shapes are finalized the mandrel is extracted from the FRP composite pipes. There are many producers of helicoidal filament winding of FRP composite pipes [18], like Amiantit Group Company, Bonstrant Ltd, Flowtite Company, Sarplast Iniziative Industriali, Future Pipe Industry, Sekisui Pipe Technology and Superlite Pipe Industries.

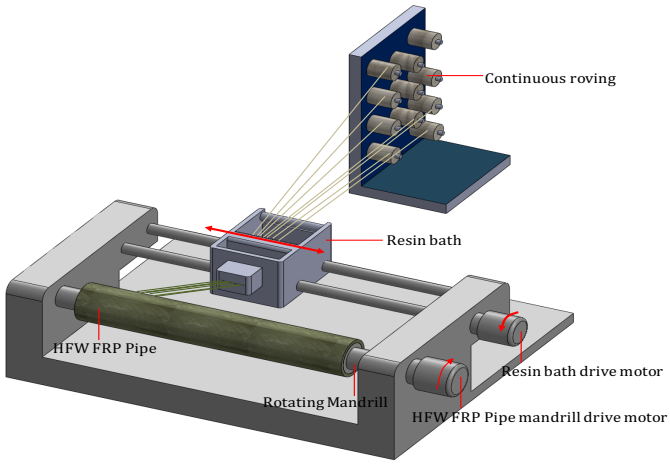

Figure 3. Helicoidal filament winding production process

The process of continuous filament winding, CFW mandrel is continuously over the cylindrical steel band as beam support. The steel band conveyed on a forward moving mandrel that can collapse and return to the beginning of the conveyor. From the side of the mandrel rotation are applied continuous fibres, chopped fibres, resins and aggregate fillers simultaneously. The FRP composite pipes shapes are drying and hardening continuously by the movement of mandrel and steel band to the standard length of FRP

composite pipes and cut by synchronized saw. There are many producers of continuous filament winding composite pipes [18], like Flowtite Technology, Amiantite Group Company.

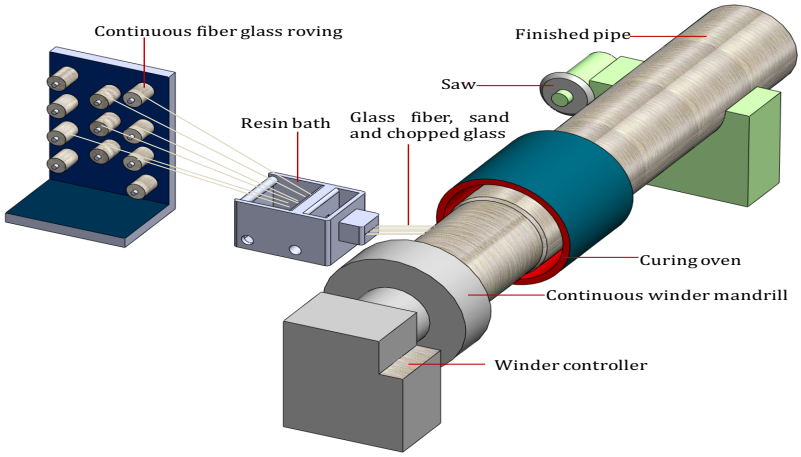

Figure 4. Continuous filament winding process

In FRP composite pipe production by centrifugal casting, the wall structures are built from the outside surface to the interior surface in a rotating mold. The mold gears simultaneously orbit, at a relatively slow speed, the centrifugal pipes raw materials (unsaturated polyester resin, reinforced glass fibres and aggregates) are precisely distributed in specific layers. The raw materials are condensed and trapped air is vented and the pipes walls are constructed from the outside inward. The final shape of pipes is heated inside the mold. Meanwhile, the mold is kept in rotation during the cure process to ensure the wall thickness over the pipes length. There are many producers of CC-FRP composite pipe like Hobas Engineering, Saudi Arabia's Amiantit, Grootint GRP System and Superlit Pipe Industries [18].

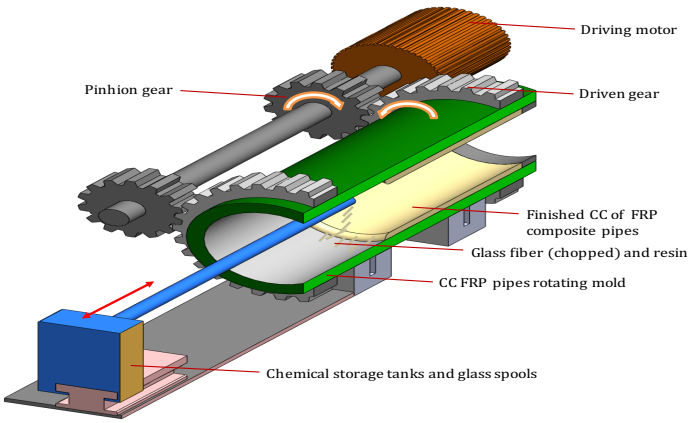

Figure 5. Centrifugal casting process of FRP composite pipe

Hybrid FRP composite pipes is a large diameter pressure pipe for structural strengthening system and the renovation of FRP composite pipes from the occurrence of failure or weakened large diameter pressure pipe [12-18]. The production system

combines an inner and outer layer of carbon or glass fibre with layers using steel wire wound reinforced.

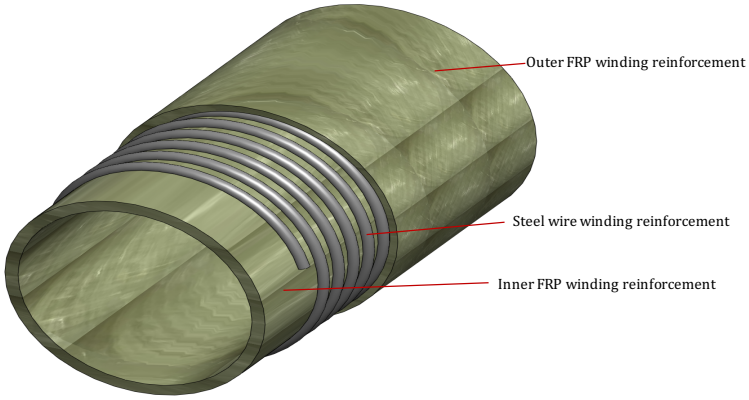

Figure 6. Hybrid production process of FRP composite pipe

2.3.2 FRP Composite Pipes Standards

Taking into account that various applications of FRP composite pipes are most relevant in chemical industry, offshore facilities, transportation system and sewage system; FRP composite pipes design is based on internal pressure for high pressure and low pressure loading condition. Generally, high pressure of FRP composite pipes are from the production types of helicoidal filament winding, HFW, with different helicoidal winding, continuous filament winding of fibres and centrifugal casting of FRP composites pipes are for lower pressure applications. Meanwhile, many FRP composite pipes production has different techniques to provide the high quality and more durable requirement to pipes standard organization.

There are several major reference organizations that develop FRP composite pipes standards, but the most common in the applications known are ASTM International, AWWA-American Water Works Association, CEN-European Committee for Standardization and ISO-International Standard Organization [1]. The purposes of FRP composite pipes standard studies are to generalize the dimension of FRP composite pipes from different materials properties. In this study of FRP composite pipes, there are several references standard of product types that can be compared:

- ASTM D3262-Standard Specification for “Fibreglass” (Glass-Fibre-Reinforced Thermoplastic-Resin) Sewer Pipe.
- ASTM D3517-Standard Specification for “Fibreglass” (Glass-Fibre-Reinforced Thermoplastic-Resin) Pressure Pipe.
- ASTM D3754-Standard Specification for “Fibreglass” (Glass-Fibre-Reinforced-Thermosetting-Resin) Sewer and Industrial Pressure Pipe.
- ASTM D2997-Standard Specification for Centrifugally Cast “Fibreglass” (Glass-Fibre-Reinforced-Thermosetting-Resin) Pipe.
- AWWA C950-Standard for Fibreglass Pressure Pipe.
- AWWA M45-Fibreglass Pipe Design Manual

- EN 1796- Plastic piping system for drainage and sewerage with or without Pressure-Glass-reinforced thermosetting plastic (GRP) based on unsaturated polyester resin (UP).
- EN 14364-Plastics piping systems for drainage and sewerage with or without Pressure-Glass-reinforced thermosetting plastics (GRP) based on unsaturated polyester resin (UP)-Specifications for pipes, fitting and joints.
- ISO 10467-Plastics piping systems for pressure and non-pressure drainage and Sewerage-Glass-reinforced thermosetting plastics (GRP) systems based on unsaturated polyester (UP) resin.
- ISO 10639-Plastics piping systems for pressure and non-pressure water Supply-Glass-reinforced thermosetting plastics (GRP) systems based on unsaturated polyester (UP) resin.
- ISO 14692-Petroleum and natural gas Industries-Glass reinforced plastics (GRP) piping.

All FRP composite pipes standards above mentioned, referred to transportation water supply systems groups are ASTM D3517, AWWA C950, EN 1796 and ISO 10639. Sewage transportation piping systems without internal pressure groups are ASTM D3262, ASTM D3754, EN 14364 and ISO 10467. In chemical industries and offshore facilities, ISO 14692 are widely used for the oil and gas industry, approving for offshore facilities AWWA M45 is used for underground pipe systems.

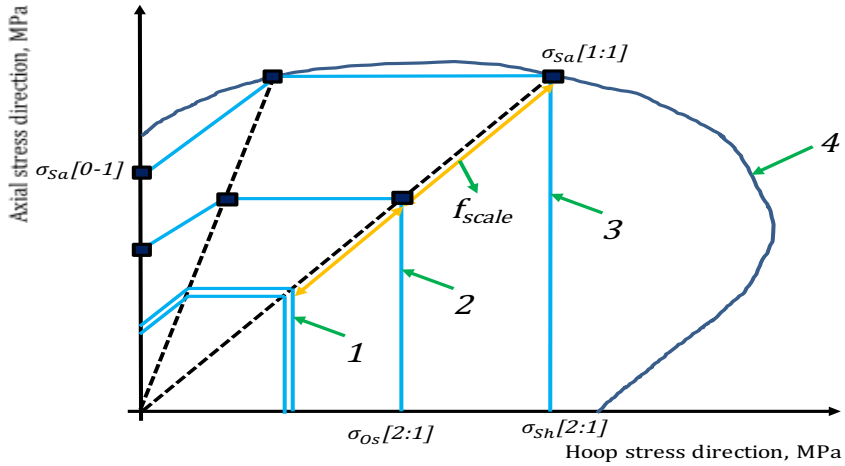

Figure 7. Idealized envelopes for a single-helicoidal wound-ply GRP pipe with HFW ranging from [45-75]°.

The pressure piping standard product for oil and gas industries by ISO 14692 and other ISO and CEN can be differentiated by the regression qualification based on a design life, the validity of normative procedure to define the factor failure envelope, considering a biaxial (circumferential plus longitudinal) stress state, the reference test temperature is at 60°C and establishes a limited (less stringent) qualification procedure for low-pressure water applications. Some standard establishes the procedures for holding the hydrostatic design basis (HDB) or the pressure-design basis (PDB) for FRP composite piping products, by appraising strength-regression data derived from pipe or fitting tests.

The data hold from the test methods is plotted as hoop stress or internal pressure versus time-to-failure relationships at the selected temperatures that simulate actual anticipated product end-use conditions. The envelopes presented in figure 7 explain three different phases as (1) Long-term design envelope, (2) idealized long-term envelopes, (3) idealized short-term envelopes, (4) schematic representation of the short-term failure envelope (after ISO 14692:2002) [8].

2.3.3 FRP Composite Pipes Properties

Physical and mechanical properties of FRP composite pipes materials are defined in this study for several production techniques of FRP composite pipes. The basic fibre materials, such as continuous roving fibres, chopped fibres, resins and additives are classified for different properties: chemical resistance, temperature resistance, abrasion resistance, flame retardants, weathering resistance, resistance to biological attack and tuberculation [1-19]. In mechanical properties, circumferential and longitudinal stress due to internal pressure, elastic modulus, failure materials, thermal coefficient of expansion, and thermal conductivity are properties to consider in order to optimize the durability issues of FRP composite pipes [1-42].

2.3.4 FRP Composite Pipes Prediction Methodology

The prediction methods of FRP composite pipes in short-term and long-term performance and durability are determined by the short-term internal pressure, tensile test and three-point bending creep test up to 10,000 hours' minimum regularly for 50 years' performance values [20-23]. Meanwhile, in this thesis the FRP composite pipes 1 hour short-term testing is used to predict creep burst pressure test in accordance to the pressure design basis for fibreglass pipe and fitting, ASTM D2992-01 is the standard specification for fibreglass pressure pipe [24], ASTM D3517-04 is for long-term of FRP composite pipes testing [25]. The creep burst pressure test experiment is associated to the short-term testing ASTM D1598-02 and ASTM D1599-99 for time to failure under constant pressure [26-27]. This method is based on the application of non-pressure FRP composite pipes and pressure FRP composite pipes by considering the required standard. Tensile test of FRP composite pipe is geometrically associated to the ASTM D3039 standard testing method for tensile properties of polymer matrix composite materials and standard testing method based on tensile properties of plastics, ASTM D638-08 [28-29].

Three-point bending creep test are predicting to 10080 minutes where geometrically associate to the ASTM D3039. The testing standard method and life prediction is based on ASTM D790-02 and ASTM D2990-01[30-31].

2.4 Failure Analysis of FRP Composite Pipes

Many researchers have been analyzing various aspects of FRP composite pipes in the demands of wide range application of FRP composite piping systems. A greater number of studies in FRP composite pipes field have evaluated the influence of FRP composite pipes production processes in helicoidal filament winding, HFW, continuous filament wound, centrifugal casting and hybrid production. Typical failures mechanism of longitudinal and circumferential loads, internal pressure, external load and failure evaluation are performed by theoretical analysis and experimental study [37,39-40].

Identification and Comparison of FRP composite pipe standard

Test/parameter	Standard											
	ASTM D3262	ASTM D3262	ASTM D3517	ASTM D3754	AWWA C950	AWWA M45	EN 1769	EN 14364	ISO 10467	ISO 10639	ISO 14692
Initial circunferential tensile strength (Failure pressure)	n/a	ASTM D1599	ASTM D1599	ASTM D1599	ASTM D1599	ASTM D1599	EN 1394	EN 1394	ISO 8521	ISO 8521	ASTM D1599
Long-term circumferential tensile strength (Failure pressure)	n/a	ASTM D2992	ASTM D2992	ASTM D2992	ASTM D2992	ASTM 2992	EN 1447	EN 1447	ISO 7509	ISO 7509	ASTM D2992
Cyclic pressure strength	n/a	n/a	n/a	ASTM D2143	ASTM D2143	ASTM D2143	EN 1638	EN 1638	ISO 15306	ISO 15306	ASTM D2143
Initial specific ring stiffness	ASTM D2412	ASTM D2412	ASTM D2412	ASTM D2412	ASTM D2412	ASTM D2412	EN 1228	EN 1228	ISO 7685	ISO 7685	ASTM D2412
Long-term specific ring stiffness	n/a		n/a	n/a	n/a	n/a	ISO 10468	ISO 10468	ISO 10468	ISO 10468	n/a
Initial ring deflection	ASTM D2412	ASTM D2412	ASTM D2412	ASTM D2412	n/a	ASTM D2412	ASTM D2412	ISO 10468	ISO 10468	ISO 10468	ASTM D2412
Long-term ring deflection	n/a	n/a	n/a	n/a	n/a	n/a	ISO 10471	ISO 10471	ISO 10471	ISO 10471	n/a
Longitudinal tensile strength	ASTM D638	ASTM D638	ASTM D638	ASTM D638	ASTM D2105	ASTM D2105	EN 1393	EN 1393	ISO 8513	ISO 8513	ASTM D2105
Methods for regression analysis of test data	n/a	(ASTM D2992)	(ASTM D2992)	(ASTM D2992)	(ASTM D2992)	(ASTM D2992)	(ASTM D2992)	ISO 10928	ISO 10928	ISO 10928	(ISO 14692)

Table 1. Pipe standards for various applications

2.5 References

1]. AWWA Manual M45, First Edition. (1999). *Fiberglass Pipe Design.* American Water Works Association.

2]. Greentech, G. (2016) "FRP Pressure Pipe". Retrieved from www.gilgwang.co.kr.

3]. Kleschinski M, Muller D, (Springer. 2005). *Composite Structures for Ocean Energy Applications.* Otto-Hahn-Strabe 5, 34123 Kassel: xperion ALPHA Composites GmbH.

4]. Beckwith S, Greenwood M, (May, 2006). Don't Overlook Composite FRP Pipe. *www.che.com*, 42.

5]. Martin R, (2008). *Aging of Composites*, The Institute of Materials, Minerals & Mining, Woodhead Publishing and Maney Publishing.

6]. Keller Michael W, Jellison B. D, Ellison T. (2013). Moisture effects on the thermal and creep performance of carbon fiber/epoxy composite for structural pipelines repair. *Elsevier Ltd*, 45, 1173-1180.

7]. Saidane, E. H, Scida D, Assarar M, Sabhi H. and Ayad R. (2016). "Hybridisation effect on diffusion kinetic and tensile mechanical behaviour of epoxy based flax–glass composites." Composites Part A: Applied Science and Manufacturing 87: 153-160.

8]. Pavlov D. G, (2013) Composite Materials in Piping Application: Design, Analysis and Optimization of Subsea and Onshore Pipelines from FRP Composites. DEStech Publication, ISBN No. 978-1-60595-029-7

9]. Gibson A. G, Ortheguy Torres M. E, Browne T.N.A, Feih S, and Mouritz A.P, (2010). High temperature and fire behaviour of continuous glass fibre/polypropylene laminates. *Composite: Part A, 41*, 1219-1231.

10]. Karpuz, P. (May, 2005). *Mechanical characterization of filament wound composite tubes by internal pressure testing.* Master thesis of Metallurgical and Materials Engineering, Middle East Technical University.

11]. Eslami, S. (May, 2013). *Durability of Perforated GFRP under various environmental conditions with emphasis on its application as a liner for directional oil wells.* Halifax, Nova Scotia: Ph. D Thesis.

12]. Baker A, Dutton S, and Kelly D, (2004). *Composite Materials for Aircraft Structure* (Second Edition ed.). American Institute of Aeronautics and Astronautics, Inc.

13]. Davies P, Boisseau A, Choqueuse D, Peters L, Renaud C, Nickel R, Thiebaud F, Perreux D, (2010). Marine Composite for Ocean Energy Application: Ensuring long-term durability. *Third International Conference on Ocean Energy.*

14]. Associates, E. G. (1999). *Marine Composites, Second Edition.* Eric Greene Associates, Inc.

15]. Guo B, Song S, Ghalambor A, and Lin T, (2014). *Offshore Pipelines (Design, Installation and Mantenance) Second Edition.* Elsevier Inc.

16]. Hoa, S. V. (2009). *Principles of the Manufacturing of Composite Materals.* DEStech Publications, Inc.

17]. Mallick, P. K. (2007). *Fiber-Reinforced Composite (Materials, Manufacturing, and Design) Third Edition.* Taylor and Francis Group, LLC.

18]. G. Marsh. (2009). Composite pipes capture water and sewage markets. *Elsevier Ltd*, 18.

19]. Guedes R. M, Sá A, and Faria H. (2007). Influence of moisture absorbtion on creep of GRP composite pipe. *Elsevier Ltd (Polymers Testing)*, 595.

20]. Kim H-Y, Y-H. Park, Y-J You and C-K. Moon (2008)."Short-term durability test for GFRP rods under various environmental conditions." Composite Structures 83(1):37-47.
21]. Na L, Sirong Z, Jianzhong C, Xi F. (2015). Long-term behavior of GFRP pipes: Optimizing the distribution of failure points during testing. *Elsevier Ltd*, 48, 7-11.
22]. Faria H, Guedes R. M. (2010). Long-term behaviour of GFRP pipes: Reducing the prediction test duration. *Elsevier Ltd*, 29, 337-345.
23]. Yoon S. H, Oh J. O, (2015). Prediction of long term performance for GRP pipes under sustained internal pressure. *Composite Structure*, 134, 185-189.
24]. D2992-01, ASTM. (2001). *Standard Practice for Obtaining Hydrostatic or Pressure Design Basis for "Fiberglass" (Glass-Fiber-Reinforced Thermosetting-Resin) Pipe and Fitting.* ASTM International.
25]. D3517-04, ASTM. (2004). *Standard Specification for "Fiberglass" (Glass-Fiber-Reinforced Thermosetting-Resin) Pressure Pipe.* ASTM International.
26]. D1598-02, ASTM. (2002). *Standard Test Method for Time-to-Failure of Plastic Pipe Under Constant Internal Pressure.* ASTM International.
27]. D1599-99, ASTM. (2000). *Standard Test Method for Resistance to Short-time Hydraulic Pressure of Plastic Pipe, Tubing, and Fitting.* ASTM International.
28]. D3039/D3039M-00, ASTM. (2000). *Standard Test Method for Tensile Properties of Polymer Matrix Composite Materials.* ASTM International.
29]. D638-08, ASTM. (2008). *Standard Test Method for Tensile Properties of Plastics.* ASTM International.
30]. D790-02, ASTM. (2002). *Standard Test Method for Flexural Properties of Unreinforced and Reinforced Plastics Electrical Insulating Materials.* ASTM International.
31]. D2990-01, ASTM. (2001). *Standard Test Method for Tensile, Compressive, and Flexural Creep and Creep-Rupture of Plastics.* ASTM International.
32]. Moser A. P, (2001). *Buried pipe Design, Second Edition.* McGraw-Hill.
33]. Dons, K. (June 2013). *Filament winding of composite tubes.* Norway: Norwegian University of Science and Technology, Mechanical Engineering, Master of Science Thesis.
34]. Hodgkinson, J. M. (2000). *Mechanical testing of advanced fibre composite.* Woodhead publishing limited Cambridge England
35]. Hossain, M. E. (2011). The current and future trends of composite materials: an experimental study. *Journal of Composite Materials*, 2133.
36]. Deniz M. E, Ozdemir O, Ozen M, and Karakuzu R. (2013). Failure pressure and impact response of glass'epoxy pipes exposed to seawater. *Elsevier, Ltd, 53*, 355-361.
37]. Abdul Majid M. S, Afendi M, Afendi P, M. Haslan, Krishnan P, Amin A. M, (2014). Ageing effects on burst pressure test of impacted glass fibre reinforcement epoxy (GRE) pipes. *Trans Tech Publications, Switzerland, 695*, 717-720.
38]. Braestrup M. W, J. B, Andersen L. W, Bryndum M, Christensen C.R, Nielsen N.J.R. (2005). *Design and Installation of Marine Pipelines.* Oxford OX4 2DQ, UK: Blackwell Science Ltd.
39]. Deolia P, Shaikh F. A, (2016). Burst pressure analysis of a pressure vessel: A review. *International Journal of Research in Advent Technology*, 2321-9637.

40]. Rafiee, R. (2016, February 18). On the mechanical performance of glass-fibre-reinforced thermosetting-resin pipes: A review. *Elsevier Ltd*, 151.
41]. Braskoro S, Dronkers T. D. T, Driel M. van, (2004). From Shallow to Deep Implications for Offshore Pipeline Design. *Indonesian Oil and Gas Community*.
42]. Bai Y, Bai Q, (2012). *Subsea Engineering Handbook.* Elsevier Inc

3. Theoretical Analysis and Experimental Study

3.1 Mechanical Properties of FRP Composite Pipes

The filament winding is being commonly used to obtain the FRP composite pipes by CNC control production with helicoidal filament winding, HFW ±45° and HFW ±55°. Three layers of helicoidal filament winding, HFW, are bonded together by unsaturated polyester resin to consider FRP composite pipes solid modeling [1]. The fibre (E-Glass) and resin (unsaturated polyester) have different specific mechanical properties, with different fibre direction of helicoidal filament winding, HFW ±45° and HFW ±55°. Then, after cure, the physical properties can be determined using the burst pressure test, tensile test and three-point bending creep tests of FRP composite pipes.

Table 2. Mechanical properties of FRP [E-glass] fibre and unsaturated polyester resin [2-3]

Properties	Unit	E-Glass	Unsaturated polyester
Elastic Modulus	E [Gpa]	72.4	3.8
Shear Modulus	G [Gpa]	30.2	4.1
Tensile strength	σ_{TS} [Gpa]	2500	70
Poisson Ratio	ν [-]	0.2	0.42
Density	$\boldsymbol{\rho}$ [g/cm^3]	2.6	1.3

Moisture behavior of FRP composite pipe in hydrology ageing process w.r.t. the FRP composite pipes weight are performed considering load [1, 4-7], time dependent, ambient temperature and temperature be at 60°C. The dimension of FRP composite pipes used in this study are presented in table 3.

Table 3. Dimensions of FRP composite pipes

Helicoidal Winding	Units	± 45°	± 55°
Average wall thickness	[mm]	3.33	4.24
Number of plies	[-]	3	3
Average length	[mm]	200	250
Average weight	[gram]	27	42

3.2 Short-Term Test Properties of FRP Composite Pipes

The characteristics of FRP composite pipes with helicoidal filament winding design are used for application in offshore pipeline, onshore pipeline, aircraft fuselage and helicopter rotor shaft [8-13]. The most complex issue of FRP composite pipes is axial tension by the fluctuation of fluid pressure, hastened by tensioner of holding clamp and lay down method [S-lay, J-lay, Reeled-lay, Towed-lay] of FRP composite pipe installation, where can be affected by the pressure damage, tension damage and bending damage at FRP composite pipes properties.

The FRP HFW composite pipes will be evaluated by four different short-term experimental tests, such as burst pressure test, creep burst pressure test, tensile testing and three-point bending creep test. The two different FRP composite pipes of HFW ±45°and HFW ±55° construction types are based on the ASTM, CEN and API standard.

The creep burst pressure tests of FRP composite pipes from different HFW ±45°and HFW ±55° were conducted in unconditioned and conditioned in water immerse, WI sea water immerse, SWI and diesel immerse, DI specimens [6]. The air pressure, pressurize the FRP

composite pipes in order to define potential damage zone and to determine the burst strength of FRP composite pipes [14-16]. The damage zone could be observed by the distinct leakage failure and damage type leakage and ruptures FRP HFW composite pipes within the time of test [14-15]. The viscoelastic strain of FRP composite pipes is related to the durability of FRP composite pipes materials under constant internal pressure for a given creep testing time and depending on environmental temperature.

Basically, the short-term experimental preparation for tensile testing and three-point bending creep test specimens are prepared from FRP composite pipes and the specimen parameters for tensile testing of FRP composite pipes of HFW ±45° and HFW ±55° are based on ASTM D3039 standard and three-point bending creep test based on ASTM D790-02 and ASTM 2990-01 [17-19]. The tensile testing and three-point bending creep test specimens are modelled in circular arc beam, being the specimens prepared in five different ageing condition: unconditioned, U specimens; water immerse, WI specimens; seawater immerse, SWI specimens and diesel immerse, DI specimens within 10080 minutes at environmental temperature and another different ageing condition are immersed in water at 60°C during 10080 minutes. The immersion time is selected to be similar to the experimental time at three-point bending creep test.

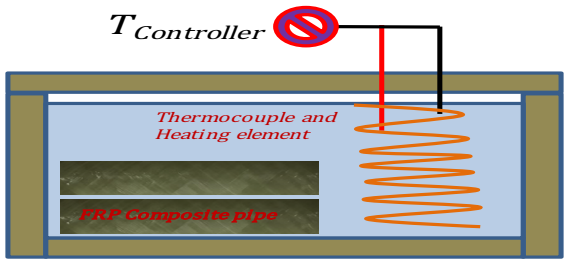

Figure 8. Schematic diagram of ageing process

Tensile testing of circular arc beam specimens is selected to get the maximum strength of FRP composite pipe HFW ±45° and HFW ±55°. The axisymmetric fibre direction will be evaluated from maximum force in tension, fibre and matrix break types from different ageing condition.

Meanwhile, for three-point bending creep testing a constant load is applied at circular arc beam specimens during the period of 10080 minutes. The instantaneous strain and viscoelastic strain, at different stress levels, of FRP composite pipes circular arc specimens are evaluated for the lifetime failure properties.

3.3 Short-Term Experimental Test

3.3.1 Burst Pressure Test of FRP Composite Pipes

The internal pressure of FRP composite pipes is hold by the two-ended light aluminum lid and fastened by eight bolts from each side. Four circular arc grips of steel with rubber are clamped to the FRP composite pipes with light aluminum lid. From burst pressure developed radial stress, tangential stress and circumferential stress. Consider that FRP composite pipe with $D/t \geq 20$ are referred to as thin-wall pipe, and the with $D/t \leq 20$ are considered as thick-wall pipe [20].

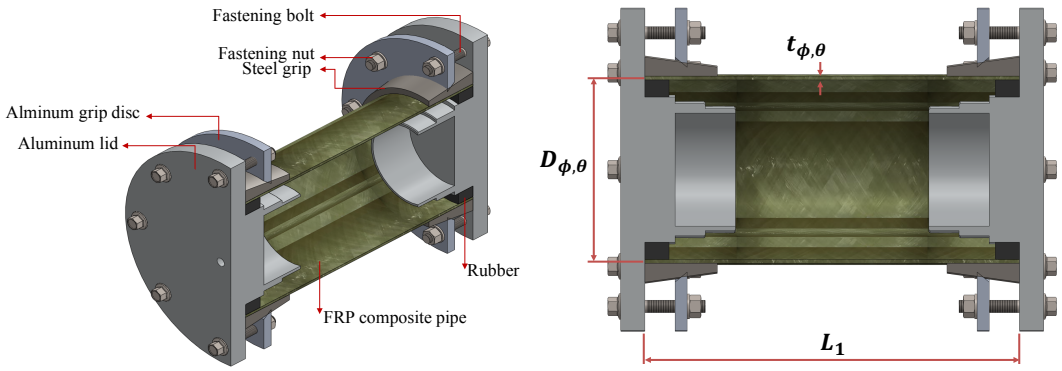

Figure 9. Setup for internal pressure of FRP composite thin pipe

Carry on, considering that internal stress of FRP composite thin pipe is $\sigma \leq \sigma_N$ nominal stress of the fastening bolts and light aluminum lid. The circumferential stress of FRP composite thin pipe of different fibre orientation is given by [1,14-15,21,28];

$$\sigma_{C_{\phi,\theta}} = \frac{F}{A_{\phi,\theta}} = \frac{P \cdot D_{\phi,\theta} \cdot L_1}{2 \cdot L_1 \cdot t_{\phi,\theta}} = \frac{P \cdot D_{\phi,\theta}}{2 \cdot t_{\phi,\theta}} \quad (1.)$$

The longitudinal stresses of FRP composite in thin-wall pipes for different fibre orientation laminates of HFW $\pm 45^{\circ}$and HFW $\pm 55^{\circ}$ are given as;

$$\sigma_{L_{\phi,\theta}} = \frac{F}{A_{\phi,\theta}} = \frac{P \cdot \frac{\pi}{4} \cdot D_{\phi,\theta}^2}{\pi \cdot D_{\phi,\theta} \cdot t_{\phi,\theta}} = \frac{P \cdot D_{\phi,\theta}}{4 \cdot t_{\phi,\theta}} \quad (2.)$$

P is the burst pressure of FRP composite thin pipe [N]

$D_{\phi,\theta}$ is diameter of FRP composite thin pipe [mm]

L_1 is length of FRP composite thin pipe [mm]

$t_{\phi,\theta}$ is thickness of FRP composite thin pipe [mm]

$\sigma_{L_{\phi,\theta}}$ is longitudinal stress [Pa]

$\sigma_{C_{\phi,\theta}}$ is circumferential stress [Pa]

F is burst force of FRP composite thin pipe [N]

$A_{\phi,\theta}$ is area of the FRP composite thin pipe [mm^2]

The unconditioned FRP composite thin pipes with different helicoidal filament winding are investigated to define the maximum burst pressure. There will be several morphological behaviors: moisture absorption, burst strength, potential damage zones, and distinct leakage failure, damage types named leakage and eruption [14]. Time dependency of creep internal pressure of FRP composite thin pipe in short-term constant internal pressure tested during 1 hour is defined by the hydrostatic or pressure design basis ASTM D2992 standard test and associated with ASTM 1598-02 time-to-failure of polymers pipe under constant internal pressure, ASTM 1599-99 test method for resistant short-time hydraulic of polymers pipe and ASTM 3517-04 Fibreglass GFRP pressure pipe [19, 22-24].

The long-term prediction hydrostatic strain is performed by linear regression analysis, based in the following equation:

$$\varepsilon_{f_{\phi,\theta}} = a + bt_{u_{\phi,\theta}} \quad (3.)$$

consider that;

$\varepsilon_{f_{\phi,\theta}}$ is variable of strain of FRP composite thin pipe failure lifetime [-]

$t_{u_{\phi,\theta}}$ is variable of time dependent FRP composite thin pipe [minutes]

a is the intercept of the strain failure lifetime axis [-]

b is the slope of the line [1/minutes]

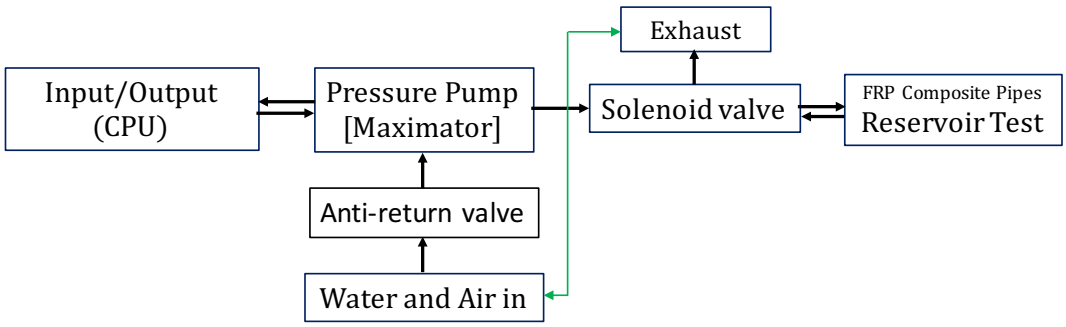

Figure 10. Diagram of burst pressure test of FRP composite pipes

The internal pressure devices were constructed by INEGI-UPorto. The devices were assembled with a solenoid valve, pressure pump (Maximator M 111-2L series maximum 220 MPa) and anti-return valve that connected to input/output [CPU unit]. Burst pressure of FRP composite pipes HFW ±45° and HFW ±55° are schematically shown as diagram in figure 10. The FRP composite pipes HFW ±45° and HFW ±55° are filled by water as reservoir test and the internal pressure of FRP composite is controlled by the CPU unit process for pressure regulator. The air and water flow through pressure pump Maximator where solenoid valve control gives signal to reservoir of internal pressure of FRP composite pipes. The excessive internal pressure by air and water flows out through the solenoid valve to exhaust.

3.3.2 Tensile Test of FRP Composite Pipes

The tensile test of circular arc beam specimens of FRP composite pipe were associated to the ASTM D 638-08 tensile properties of polymers and ASTM D 3039 tensile properties of polymers matrix composite materials [17,25]. In general, the specimens have two different helicoidal filament winding, HFW ±45˚and HFW ±55˚ of FRP pipe, where the specimens were prepared by different ageing: unconditioned, U water immerse, WI sea water immerse, SWI and diesel immerse, DI during 10080 minutes at ambient temperature and water immersion at 60˚C. The tests were conducted with five different types of specimens: U specimens, WI specimens, SWI specimens, DI specimens and WI specimens at 60°C within 10080 minutes. An universal testing machine with capacity 120 kN, as seen in figure 11, was used to carry out the FRP composite pipe specimens tensile test. The specimens were loaded under displacement control with loading rate of 2.0 mm/min until the failure occurred. The unconditioned, U, specimens test were carried out for three specimens for an average mechanical property and different ageing conditioned specimens in WI, SWI and DI were carried out for each test specimen.

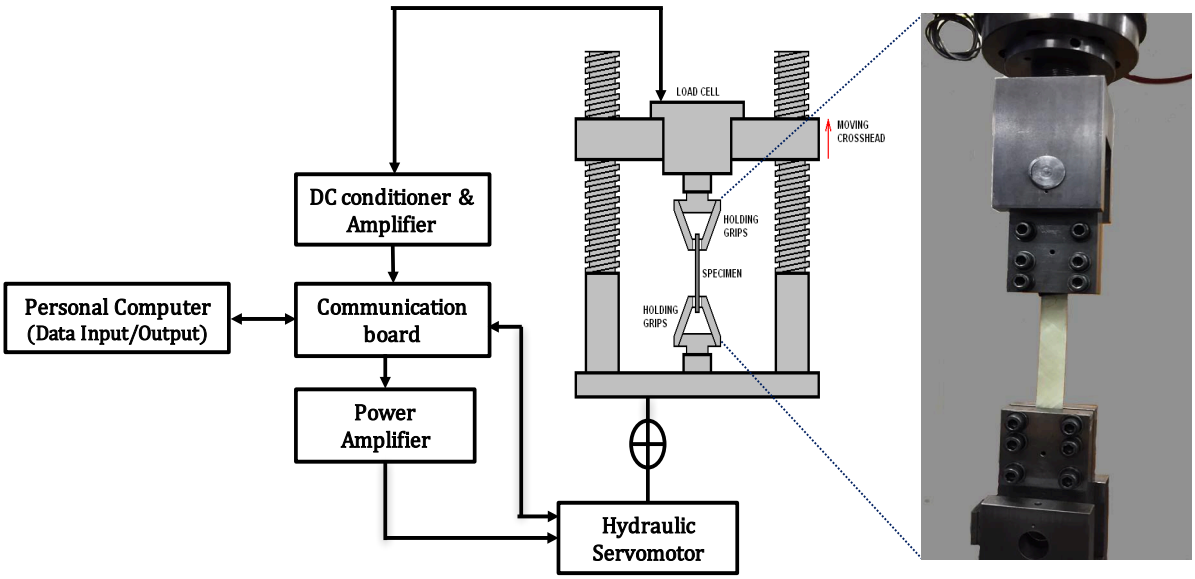

Figure 11. Schematic diagram of tensile test

FRP composites thin pipe tensile test for unconditioned and conditioned specimens are obtained from FRP composite thin pipe section with different HFW $\pm 45^{\circ}$ and HFW $\pm 55^{\circ}$in circular arc beam shape. The circular arc beam length is defined by the angle of radian β that is divided by two at radius of circular arc beam length.

The unconditioned and conditioned circular arc beam specimens are gripped at the end shape by circular arc beam holding grips. For the symmetric directions of filament winding in a circular arc beam specimen of FRP composite thin pipe the maximum tensile stress are defined as [17]:

$$\sigma_{Max_{\phi,\theta}} = \frac{F}{A_{\phi,\theta}} \tag{4.}$$

and

the maximum tensile strain;

$$\varepsilon_{Max_{\phi,\theta}} = \frac{\Delta L}{L_o} = \frac{L - L_o}{L_o} \tag{5.}$$

Consider that area of the circular arc beam specimen of FRP composite pipes are [26];

$$A_{\phi,\theta} = 2 \cdot \beta \cdot r \cdot t_{\phi,\theta} \tag{6.}$$

Being θ, the angle for a given circular arc beam length, $b_{\phi,\theta}$ is obtained [27];

$$b_{\phi,\theta} = \pi \cdot r \cdot \frac{\theta}{180^{\circ}};\ \theta = \frac{b_{\phi,\theta} \cdot 180^{\circ}}{\pi \cdot r}; \beta = \frac{\theta}{2} \tag{7.}$$

Standard test method measurement was performed following the ASTM D638-08 and ASTM D3039 for FRP composite thin pipe circular arc beam specimen tensile test. The FRP helicoidal filament winding pipe specimens WI at 60˚C are released 25 minutes before setup to the tensile test machine. Finally, the test results will be looked for maximum stress and maximum strain from different HFW of FRP in different application from different ageing.

3.3.3 Three-Point Bending Creep Test of FRP Composite Pipes

Three-point bending of FRP composite thin pipe are selected to explore the viscoelastic properties of fibre and matrix of FRP HFW composite pipe from external loading that occur on FRP composite thin pipe in lay down method during the period under loading. As the application in the deep sea water level phenomena, underground installation for FRP composite pipe, the three-point bending case has high consideration in this study.

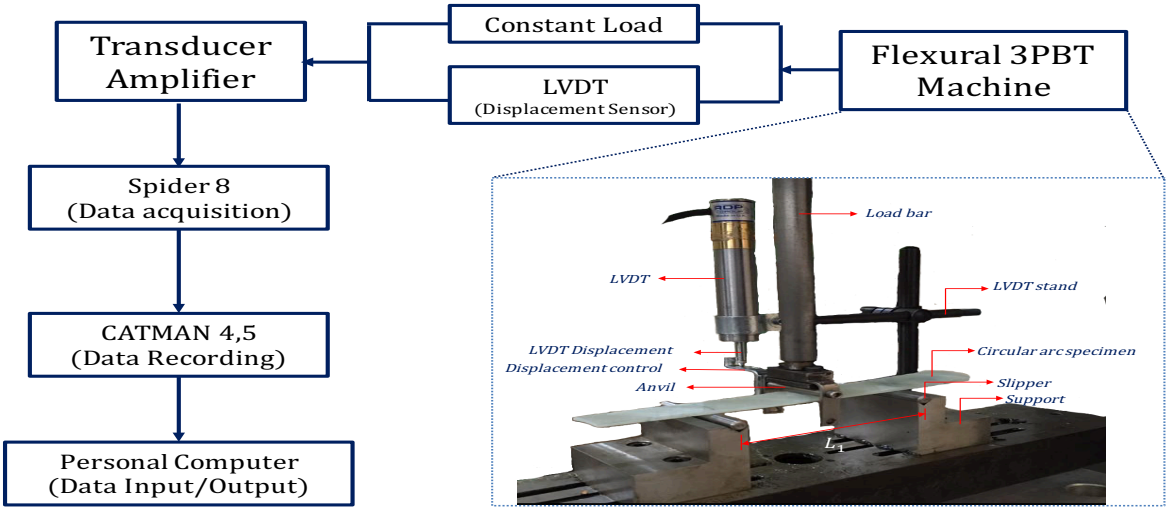

Figure 12. Three-point bending creep test schema

The unconditioned circular arc beam specimens of FRP HFW composite pipe are mounted on roller at support base with the distance of length, L_1. The constant load bar is applied by anvil contact on surface of circular arc beam specimens, HFW $\pm 45^{\circ}$ and HFW $\pm 55^{\circ}$, of FRP composite pipe from the cantilever arm that pushes the load bar. The specimen displacement, $D_{\phi,\theta}(t)$, move to maximum depth deflection with LVDT sensor simultaneously with the constant load bar. LVDT sensor record the displacement data under constant load for the time dependent three-point bending creep test of FRP composite pipe displacement. The LVDT sensor records data and transmit to the transducer amplifier Spider 8 data acquisition that stores the displacement, $D_{\phi,\theta}(t)$ and three-point bending creep test data to the output by the CATMAN 4,5 software.

The maximum stress bending of FRP composite thin pipe circular arc beam definition could be expressed by;

$$\sigma_{Max_{\phi,\theta}} = \frac{F \cdot L_1 \cdot sin\beta}{4 \cdot \beta \cdot r^2 \cdot t_{\phi,\theta}(\beta + sin\beta \cdot cos\beta)} \tag{8.}$$

$\sigma_{Max_{\phi,\theta}}$ is the stress for three-point bending creep test [MPa]

$$\sigma_{Max} = \frac{M \cdot y}{I}$$

Where [27];

σ_{Max} is maximum stress [MPa]

The strain for three-point bending creep test;

$$\varepsilon_{\phi,\theta} = \frac{12 \cdot D_{\phi,\theta}(t) \cdot r \cdot sin\beta}{L_1^2 \cdot \beta} \tag{9.}$$

The inertia of circular arc beam of FRP composite pipes [25];

$$I = r^3 t(\beta + sin\beta \cdot cos\beta) \tag{10.}$$

$$y = \frac{r \cdot sin\beta}{\beta}$$

Creep compliance for three-point bending test;

$$J_{\phi,\theta}(t) = \frac{\varepsilon_{\phi,\theta}}{\sigma_{\phi,\theta}} = \frac{\frac{12 \cdot D(t) \cdot r \cdot sin\beta}{L^2 \cdot \beta}}{\frac{F \cdot L \cdot sin\beta}{4 \cdot \beta \cdot r^2 \cdot t(\beta + sin\beta \cdot cos\beta)}} = \frac{28 \cdot D_{\phi,\theta}(t) \cdot r^3 \cdot t_{\phi,\theta} \cdot (\beta + sin\beta \cdot cos\beta)}{F_{\phi,\theta} \cdot L_1^2} \tag{11.}$$

Where, M is bending moment, y is distance at center of the beam, I is the inertia moment, r is the radius of circular arc beam, L_1 is distance of the roller circular arc beam support as shown in the schematic figure 13.

The test method for three-point bending creep test is associated to the ASTM D 2990-01 standard test methods for three-point bending creep testing [21]. The selection of the test conditions for this case, were the failure of HFW FRP composite pipes circular arc beam specimens occurs in less than 1000 hours in three-point bending creep test and the stress level was not considered as based on standard creep test. Therefore, in this experiment the loads can be configured at three different stress levels: 1%, 1,4% and 1,8% by the calculation from rupture tensile test to reduce the deflection velocity under three-point bending creep test [29,30]. The geometry of the circular arc beam specimens is based on ASTM: D 3039/D 3039M and the intention of this geometry is to uniform the dimension of circular arc beam specimens of polymers matrix composite HFW tensile test and three-point bending creep test.

Furthermore, ASTM: D790-02 standard test for flexural properties of unreinforced and reinforced polymers is followed where the test procedure is, mainly, the deflection of specimen, $d_y \leq$ circular arc beam length of specimen, $b_{\phi,\theta}$.

The specimens are unconditioned and conditioned in WI, SWI and DI at ambient temperature. Another specimen conditioned in WI at 60°C was also used in the three-point bending creep test. The period of specimens conditioning for WI, SWI and DI at ambient temperature and WI at 60°C has been 10080 minutes.

Three-point bending creep tests followed at three different constants stress level configuration for a different HFW $\pm 45^{\circ}$ and HFW $\pm 55^{\circ}$ circular arc beam. The circular arc beam will deform instantaneously under the constant load, from viscoelastic to the viscoplastic for period of 10080 minutes. The existence of linearity and nonlinearity from the constant load for the experimental period has been defined by the HFW effect of circular arc beam FRP composite pipe from unconditioned and conditioned in WI, SWI and DI at ambient temperature and conditioned in WI at 60°C.

Consider that the creep stress loading of FRP HFW composite thin pipe for the constant loading at the circular arc beam will be obtained from the loads configuration of the circular arc beam rupture tensile stress. The percentage of loading to the three-point bending creep test of HFW $\pm 45^{\circ}$ rupture tensile stress is $F_{Max} \leq 1{,}8\%$. Meanwhile, in the configuration loads for three-point bending creep test of HFW $\pm 55^{\circ}$ the rupture tensile stress will be applied for three different loads configuration w.r.t. rupture tensile strength, such as; $F_{Max} \leq 1\%$, $F_{Max} \leq 1{,}4\%$ and $F_{Max} \leq 1{,}8\%$. The load configuration has the intention to reduce the velocity of circular arc beam deflection to the time dependent of FRP composite pipe from constant loads [31].

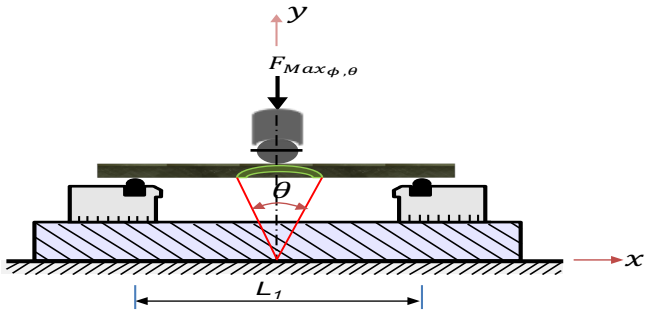

Figure 13. Three-point bending creep test illustration

By changing equation 8, the definition of maximum loads at three-point bending creep test could be as;

$$F_{Max_{\phi,\theta}} = \frac{\sigma_{Max_{\phi,\theta}} \cdot \left(4 \cdot \beta \cdot r^2 \cdot t_{\phi,\theta} \cdot (\beta + sin\beta \cdot cos\beta)\right)}{L_1 \cdot sin\beta} \tag{12.}$$

Testing method for short-term behavior FRP composite pipe, optimized the distribution of failure point from the 10080 minutes testing data. The regression analysis is performed by a prediction model for 50 years, but the regression parameter for this experimental data will be gathered for 1000 hours. The ASTM D2990-01 describes the logarithmic regression analysis of the experimental standard test method that will be presented. The log-log model of the FRP composite pipe HFW $\pm 45°$ and HFW $\pm 55°$ failure of three-point bending creep strain vs failure lifetime is defined as follows [29,30];

$$\log\left(\varepsilon_{f_{\phi,\theta}}\right) = b_{1_{\phi,\theta}} + b_{2_{\phi,\theta}} \log\left(t_u\right) \tag{13.}$$

$\log\left(\varepsilon_{f_{\phi,\theta}}\right)$ is strain at failure lifetime for three-point bending creep test [-]

$b_{1_{\phi,\theta}}$ is intercept of strain failure lifetime for three-point bending creep test [-]

$b_{2_{\phi,\theta}}$ is slope of failure lifetime for three-point bending creep test [1/minutes]

$\log\left(t_u\right)$ is time to failure for three-point bending creep test [minutes]

The FRP HFW $\pm 45°$ and HFW $\pm 55°$ are conditioned in different ageing and at different stress levels, therefore the logarithmic analysis model for three-point bending creep test of FRP composite pipe will be performed as specific logarithmic equation model in data regression analysis.

3.4 Parametric Study of Short-Term Test of FRP Composite Pipes

3.4.1 Burst Pressure of FRP Composite Pipes

Internal pressure of FRP composite pipes HFW ±45° and HFW ±55° are realized in two different experiments. The internal pressure until the diameter of FRP composite pipes is damaged and creep internal pressure of FRP composite pipes for time dependent rupture during 1 hour to obtain the maximum stress damage and maximum strain damage of FRP composite HFW ±45° and HFW ±55°. The FRP composite pipes arranged in unconditioned tubes for each HFW ±45° and HFW ±55° are provided in two tubes for experimental testing [32].

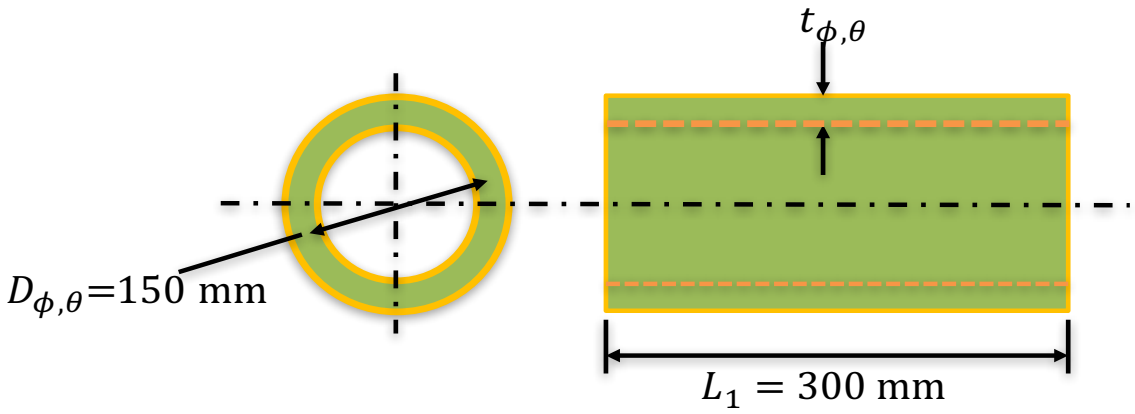

Figure 14. Geometry of FRP composite pipe tube

Specifically, maximum hoop stress and maximum longitudinal stress of HFW ±45° length, L_1= 300 mm, diameter, D_ϕ= 150 mm and average thickness, t_ϕ= 3,33 mm could be defined as;

The maximum hoop stress, $\sigma_{CMax_\phi} = \frac{P \cdot D_\phi}{2 \cdot t_\phi} = \frac{P \cdot 150mm}{2 \cdot 3{,}33mm}$

The maximum longitudinal stress, $\sigma_{LMax_\phi} = \frac{P \cdot D}{4 \cdot t_\phi} = \frac{P \cdot 150\ mm}{4 \cdot 3{,}33mm}$

Where;
P is internal air pressure [MPa]
HFW ±55° average thickness 4,24 mm could be defined as;

The maximum hoop stress, $\sigma_{CMax_\theta} = \frac{P \cdot D_\theta}{2 \cdot t_\theta} = \frac{P \cdot 150}{2 \cdot 4{,}24mm}$

The maximum longitudinal stress, $\sigma_{LMax_\theta} = \frac{P \cdot D_\theta}{4 \cdot t_\theta} = \frac{P \cdot 150\ mm}{4 \cdot 4{,}24mm}$

Regarding the long term aspects of the time dependence of FRP composite pipe HFW ±45° and HFW ±55°, the test was not performed because the experiment was not possible.

Therefore, linear regression analysis of internal pressure of composite pipe equation also was not performed within this context.

3.4.2 Tensile Test of FRP Composite Pipes

The FRP composite pipe tensile test parameter are differentiated in two types of HFW ±45° of FRP composite pipe with the specimen testing length 115 mm, circular arc beam 24 mm and average thickness of beam 3,33 mm [33]. The HFW ±55° of FRP composite pipe specimen has length 115 mm, circular arc beam 24 mm and thickness 4,24 mm.

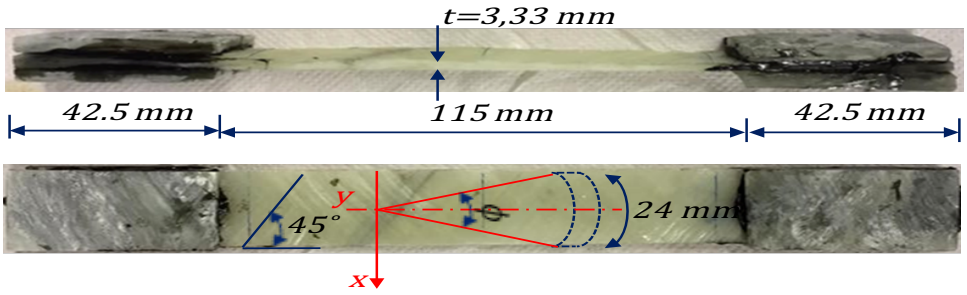

Figure 15. FRP composite pipes specimen HFW ±45°

$$\sigma_{Max_\phi} = \frac{F_{Max_\phi}}{A_\phi} = \frac{F_{Max_\phi}}{2 \cdot \beta \cdot r \cdot t_\phi} = \frac{F_{Max_\phi}}{2 \cdot 0{,}157 \cdot 75\ mm \cdot 3{,}33\ mm}$$

The specimen parameters of different HFW ±45° and HFW ±55° by different ageing at ambient temperature and 60°C are defined as shown in the table 4.

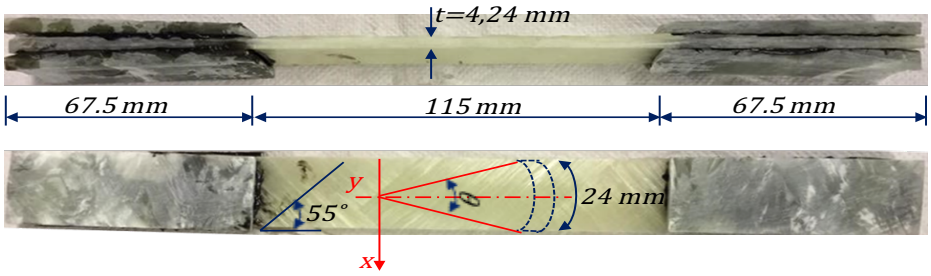

Figure 16. FRP composite pipes specimen HFW ±55°

$$\sigma_{Max_\theta} = \frac{F_{Max_\theta}}{A_\theta} = \frac{F_{Max_\theta}}{2 \cdot \beta \cdot r \cdot t_\theta} = \frac{F_{Max_\theta}}{2 \cdot 0{,}157 \cdot 75\ mm \cdot 4{,}24\ mm}$$

Stress and strain of different HFW and different ageing of FRP composite pipe materials are defined by equation 4 and equation 5. Considering the area of circular arc beam specimens of FRP composite pipe defined by equation 6, therefore the length of circular arc beam specimen is 24 mm and solved mathematically, the geometry of circular arc beam length, $b_{\phi,\theta}$, is given by equation 7 to obtain the semicircular angle, β of circular arc beam specimen of FRP composite pipe [34]. The semicircular angle, β of beam is defined by $\beta = \frac{\theta}{2}, \beta = \frac{18}{2}$ so $\beta = 9^\circ = 0{,}157$ radians.

This semicircular angle, β, result is substituted in equation 6 to obtain the area of circular arc beam specimens. By this calculation procedure, the maximum stress and maximum

strain of tensile test of FRP composite pipe from specimens with different HFW ±45° and HFW ±55°, unconditioned and conditioned specimens in different ageing treatment for WI, SWI and DI during 10080 minutes, at ambient temperature and at 60°C, could be discussed more deeply considering the maximum tensile stress of different HFW of FRP composite pipes and fibre and matrix fracture types that will occur in HFW of FRP composite pipes.

Table 4. The parameters and conditioning of FRP HFW ±45° and HFW ±55° tensile test specimens.

No.	Specimens	HFW	Parameters				Ageing		
			t	b	r	L_1	Condition	Temperature	Duration
			[mm]	[mm]	[mm]	[mm]		[°C]	[min]
1	P1V45TT	45°	3,33	24	75	115	Unconditioned	Ambient	[-]
2	P3V45TT	45°					Unconditioned	Ambient	[-]
3	P4V45TT	45°					Unconditioned	Ambient	[-]
4	P6SWI45TT	45°					Sea water immerse	Ambient	10080
5	P7D45TT	45°					Diesel immerse	Ambient	10080
6	P12W45	45°					Water immerse	Ambient	10080
7	P9W45TT-T60	45°					Water immerse	60	10080
8	P15W45TT-T60	45°					Water immerse	60	10080
9	P1V55TT	55°	4,24	24	75	115	Unconditioned	Ambient	[-]
10	P15V55TT	55°					Unconditioned	Ambient	[-]
11	P16V55TT	55°					Unconditioned	Ambient	[-]
12	P3D55TT	55°					Sea water immerse	Ambient	10080
13	P5W55TT	55°					Diesel immerse	Ambient	10080
14	P8SWI55TT	55°					Water immerse	Ambient	10080
15	P6W55TT-T60	55°					Water immerse	60	10080

3.4.3 Three-Point Bending Creep Test of FRP Composite Pipes

The ageing process of HFW ±45° and HFW ±55° of FRP composite pipe is immersion for 10080 minutes except unconditioned circular arc beam specimens. The constant applied load of HFW ±45° is 60,582 N for circular arc beam in different ageing condition at ambient temperature and at 60°C. Meanwhile, the load application to the HFW ±55° of FRP composite pipe circular arc beam for ageing condition in sea water immersion uses different applied loads, such as 100,907 N, 141,270 N and 181,632 N.

Table 5. Geometry of FRP composite pipes HFW ±45° and HFW ±55° for three-point bending creep test.

No.	Specimens	HFW	Parameters				Ageing		
			t	b	r	L_1	Condition	Temperature	Duration
			[mm]	[mm]	[mm]	[mm]		[°C]	[min]
1	P5V453PBT	45°	3,33	24	75	115	Unconditioned	Ambient	[-]
2	P10SWI453PBT	45°					Sea water immerse	Ambient	10080
3	P13D453PBT	45°					Diesel immerse	Ambient	10080
4	P8W453PBT	45°					Water immerse	Ambient	10080
5	P11W453PBT-T60	45°					Water immerse	60	10080
6	P14V553PBT	55°	4,24	24	75	115	Unconditioned	Ambient	[-]
7	P4SWI553PBT	55°					Sea water immerse	Ambient	10080
8	P10SWI553PBT	55°					Sea water immerse	Ambient	10080
9	P11SWI553PBT	55°					Sea water immerse	Ambient	10080
10	P7D553PBT	55°					Diesel immerse	Ambient	10080
11	P13W553PBT	55°					Water immerse	Ambient	10080
12	P7W553PBT-T60	55°					Water immerse	60	10080

The circular arc beam specimens immersed in water at 60°C will release absorption heat from the immersion during 25 minutes before set-up to the experimental three-point bending creep test for HFW ±45° and HFW ±55° of FRP composite pipe. The three-point bending creep specimen length is 115 mm and distance length to the center point is 50 mm. The maximum deflection of the circular arc beam specimen is $d_y \leq 24$ mm at the circular arc beam deflection deep. The experiment is conducted with constant load, therefore loads could be obtained by the rupture tensile stress HFW of FRP composite pipe tensile test and geometry of the circular arc beam. Three-point bending creep test experimental geometry of the circular arc beam of HFW ±45° and HFW ±55° can be seen in table 5.

In the HFW ±45° of FRP composite pipe, the applied constant load could be configured to 1,8%, because this load configuration is very precise to get experimental data for the maximum bending load 60,582 N. The applied load is equal to 6 kg when convert to cantilever load bar as shown in figure 12 of three-point bending creep test by the calculation using equation 12 as below.

$$F_{Max_\phi} = \frac{\sigma_{Max_\phi} \cdot (4 \cdot \beta \cdot r^2 \cdot t_\phi \cdot (\beta + sin\beta \cdot cos\beta))}{L_1 \cdot sin\beta}$$

$$F_{Max_\phi} = \frac{0{,}258\ MPa \cdot \left(4 \cdot 0{,}157 \cdot (75\ mm)^2 \cdot 3{,}33\ mm \cdot (0{,}157 + 0{,}156 \cdot 0{,}988)\right)}{100\ mm \cdot 0{,}156}$$

$$F_{Max_\phi} = 60,582\ N$$

Circular arc beam of FRP composite pipe HFW ±45° had load applied during 10080 minutes. The instantaneous deflection and time dependent deflection will define the elastic and viscoelastic of HFW ±45° FRP composite pipe for unconditioned and conditioned, at ambient temperature and at 60°C, with stress and strain calculation by equation 8. So, the three-point bending creep test by maximum stress σ_{Max_ϕ} for constant loading is;

$$\sigma_{Max_\phi} = \frac{F_{Max_\phi} \cdot L_1 \cdot sin\beta}{4 \cdot \beta \cdot r^2 \cdot t_\phi (\beta + sin\beta \cdot cos\beta)}$$

$$\sigma_{Max_\phi} = \frac{60{,}582N \cdot 100\ mm \cdot 0{,}156}{4 \cdot 0{,}157 \cdot (75\ mm)^2 \cdot 3{,}33\ mm(0{,}157 + 0{,}156 \cdot 0{,}988)}$$

$$\sigma_{Max_\phi} = 0{,}258\ MPa$$

Time dependent strain, ε_ϕ at stress level configuration 1,8%, $\sigma_{Max_\phi} = 0{,}258\ MPa$ for FRP HFW ±45° specimens P5V453PBT, P10SWI453PBT, P13D453PBT, P8W453PBT, P11W453PBT-T60 is;

$$\varepsilon_\phi = \frac{12 \cdot D_\phi(t) \cdot r \cdot sin\beta}{L_1^2 \cdot \beta} = \frac{12 \cdot D_\phi(t) \cdot 75mm \cdot 0{,}156}{(100\ mm)^2 \cdot 0{,}157} = \frac{D_\phi(t) \cdot 141\ mm}{1571}$$

$D_\phi(t)$ is the time dependent deflection. Therefore, strain for the three-point bending creep test is shown graphically in figure 24. Three-point bending creep compliance of circular arc beam HFW $\pm 45°$ could be shown graphically in the figure 27.

$$J_\phi(t) = \frac{\varepsilon_\phi}{\sigma_\phi} = \frac{28 \cdot D_\phi(t) \cdot r^3 \cdot t_\phi \cdot (\beta + sin\beta \cdot cos\beta)}{F \cdot L^3}$$

$$J_\phi(t) = \frac{28 \cdot D_\phi(t) \cdot (75\ mm)^3 \cdot 3{,}33mm \cdot (0{,}157 + 0{,}156 \cdot 0{,}988)}{60{,}582\ N \cdot (100\ mm)^3}$$

$$J_\phi(t) = \frac{12256514\ mm \cdot D_\phi(t)}{60580283\ N}$$

Continue the experiments for three-point bending creep test HFW $\pm 55°$ of FRP composite pipe circular arc by beam applying several different constant stress levels, such as: 0,338 MPa [1%] 0,473 MPa [1,4%] and 0,609 MPa [1,8%]. So, this stress level 0,338 MPa [1%] will apply for circular arc beam specimen with immersion in sea water; P11SWI553PBT at ambient temperature. The stress level 0,473 MPa [1,4%] will apply for all circular arc beam HFW $\pm 55°$ and the stress level 0,609 MPa [1,8%] will apply for P4SWI553PBT specimen only.

The stress level, $\sigma_{Max_\theta} = 0{,}338$ MPa or equal to 1% configuration of the load for SWI specimen P11SWI553PBT at ambient temperature, F_{Max_θ} is calculated as;

$$F_{Max_\theta} = \frac{\sigma_{Max_\theta} \cdot (4 \cdot \beta \cdot r^2 \cdot t_\theta \cdot (\beta + sin\beta \cdot cos\beta))}{L_1 \cdot sin\beta}$$

$$F_{Max_\theta} = \frac{0{,}338\ MPa \cdot (4 \cdot 0{,}157 \cdot (75\ mm)^2 \cdot 4{,}24\ mm \cdot (0{,}157 + 0{,}156 \cdot 0{,}988))}{100\ mm \cdot 0{,}156}$$

$$F_{Max_\theta} = 181{,}632\ N$$

Time dependent strain, ε_θ at stress level, $\sigma_{Max_\theta} = 0{,}338$ MPa or equal 1% configuration for specimen P11SWI553PBT at ambient temperature is;

$$\varepsilon_\theta = \frac{12 \cdot D_\theta(t) \cdot r \cdot sin\beta}{L_1^2 \cdot \beta} = \frac{12 \cdot D_\theta(t) \cdot 75\ mm \cdot 0{,}156}{(100\ mm)^2 \cdot 0{,}157} = \frac{141\ mm \cdot D_\theta(t)}{1571}$$

$D_\theta(t)$ is the time dependent deflection. Therefore, strain for the three-point bending creep test will show as graphically in figure 25.

The creep compliance of HFW $\pm 55°$ of three-point bending creep test circular arc beam specimens for stress level, $\sigma_{Max_\theta} = 0{,}338$ MPa or equal to 1% configuration of the load for SWI specimen P11SWI553PBT at ambient temperature defined as;

$$J_\theta(t) = \frac{\varepsilon_\theta}{\sigma_\theta} = \frac{28 \cdot D_\theta(t) \cdot r^3 \cdot t_\theta \cdot (\beta + sin\beta \cdot cos\beta)}{F \cdot L_1^2}$$

$$J_\theta(t) = \frac{28 \cdot D_\theta(t) \cdot (75\ mm)^3 \cdot 4{,}24\ mm \cdot (0{,}157 + 0{,}156 \cdot 0{,}988)}{100{,}907\ N \cdot (100\ mm)^3}$$

$$J_\theta(t) = \frac{15605891{,}5\ mm^5 \cdot D_\theta(t)}{100907477{,}2\ Nmm^3}$$

Three-point bending creep compliance of circular arc beam HFW $\pm 55°$ for SWI specimen P11SWI553PBT is shown graphically in the figure 28.

The stress level, $\sigma_{\mathrm{Max}_\theta} = 0{,}473$MPa equal to 1,4 % configuration of the load, apply for specimens P14V553PBT, P10SWI553PBT, P7D553PBT and P13W553PBT circular arc beam helicoidal filament winding $\pm 55°$ is calculated as;

$$F_{Max_\theta} = \frac{\sigma_{Max_\theta} \cdot (4 \cdot \beta \cdot r^2 \cdot t_\theta \cdot (\beta + sin\beta \cdot cos\beta))}{L_1 \cdot sin\beta}$$

$$F_{Max_\theta} = \frac{0{,}473\ MPa \cdot (4 \cdot 0{,}157 \cdot (75\ mm)^2 \cdot 4{,}24\ mm \cdot (0{,}157 + 0{,}156 \cdot 0{,}988))}{100\ mm \cdot 0{,}156}$$

$$F_{Max_\theta} = 141{,}270\ N$$

Time dependent strain, ε_θ at stress level, $\sigma_{Max_\theta} = 0{,}473$ MPa or equal 1,4 % configuration is;

$$\varepsilon_\theta = \frac{12 \cdot D_\theta(t) \cdot r \cdot sin\beta}{L_1^2 \cdot \beta} = \frac{12 \cdot D_\theta(t) \cdot 75\ mm \cdot 0{,}156}{(100\ mm)^2 \cdot 0{,}157} = \frac{141\ mm \cdot D_\theta(t)}{1571}$$

$D_\theta(t)$ is the time dependent deflection. Therefore, strain for the three-point bending creep test at stress level configuration $\sigma_{Max_\theta} = 0{,}473$ MPa is shown graphically in figure 25.

Creep compliance, $J_\theta(t)$[1/MPa] in circular arc beam three-point creep test of HFW $\pm 55°$ is calculated as;

$$J_\theta(t) = \frac{\varepsilon_\theta}{\sigma_\theta} = \frac{28 \cdot D_\theta(t) \cdot r^3 \cdot t_\theta \cdot (\beta + sin\beta \cdot cos\beta)}{F \cdot L_1^2}$$

$$J_\theta(t) = \frac{28 \cdot D_\theta(t) \cdot (75\ mm)^3 \cdot 4{,}24\ mm \cdot (0{,}157 + 0{,}156 \cdot 0{,}988)}{141{,}270\ N \cdot (100\ mm)^3}$$

$$J_\theta(t) = \frac{15605891{,}5\ mm^5 \cdot D_\theta(t)}{141270468{,}1\ Nmm^3}$$

Three-point bending creep compliance of circular arc beam HFW $\pm 55°$ for SWI specimen P14V553PBT, P10SWI553PBT, P7D553PBT and P13W553PBT can be seen graphically in figure 28.

For the stress level, $\sigma_{\mathrm{Max}_\theta} = 0{,}609$ MPa or equal 1,8 % configuration of the load applied for specimens P4SWI553PBT, circular arc beam helicoidal filament winding $\pm 55°$ the maximum load calculated as;

$$F_{Max_\theta} = \frac{\sigma_{Max\theta} \cdot (4 \cdot \beta \cdot r^2 \cdot t_\theta \cdot (\beta + sin\beta \cdot cos\beta))}{L_1 \cdot sin\beta}$$

$$F_{Max_\theta} = \frac{0{,}609\ MPa \cdot (4 \cdot 0{,}157 \cdot (75\ mm)^2 \cdot 4{,}24\ mm \cdot (0{,}157 + 0{,}156 \cdot 0{,}988))}{100\ mm \cdot 0{,}156}$$

$$F_{Max_\theta} = 181{,}632\ \mathrm{N}$$

The time dependent strain, ε_θ, at stress level, $\sigma_{Max_\theta} = 0{,}609$ MPa or equal 1,8 % configuration for specimen P4SWI553PBT is;

$$\varepsilon_\theta = \frac{12 \cdot D_\theta(t) \cdot r \cdot sin\beta}{L_1^2 \cdot \beta} = \frac{12 \cdot D_\theta(t) \cdot 75\ mm \cdot 0{,}156}{(100\ mm)^2 \cdot 0{,}157} = \frac{141\ mm \cdot D_\theta(t)}{1571}$$

$D_\theta(t)$ is time dependent deflection. Therefore, strain for the three-point bending creep test at stress level configuration $\sigma_{Max_\theta} = 0{,}609$ MPa or equal 1,8 % is shown graphically in figure 26.
Creep compliance, $J_\theta(t)$[1/MPa] in circular arc beam for three-point creep test of HFW $\pm 55°$ is calculated as;

$$J_\theta(t) = \frac{\varepsilon_\theta}{\sigma_\theta} = \frac{28 \cdot D_\theta(t) \cdot r^3 \cdot t_\theta \cdot (\beta + sin\beta \cdot cos\beta)}{F \cdot L_1^2}$$

$$J_\theta(t) = \frac{28 \cdot D_\theta(t) \cdot (75\ mm)^3 \cdot 4{,}24\ mm \cdot (0{,}157 + 0{,}156 \cdot 0{,}988)}{181{,}632\ N \cdot (100\ mm)^3}$$

$$J_\theta(t) = \frac{15605891{,}5\ mm^5 \cdot D_\theta(t)}{181633459\ Nmm^3}$$

Three-point bending creep compliance of circular arc beam HFW $\pm 55°$ for SWI specimen P4SWI553PBT can be seen graphically in figure 29.

3.5 References

1]. AWWA Manual M45, First Edition. (1999). *Fiberglass Pipe Design.* American Water Works Association.

2]. Industriale, S. (2010) "SIR INDUSTRIALE". Ritrieved from www.sirindustriale.com

3]. Scorning, O. (2017) "Owenscorning". Ritrieved from www.owenscorning.com

4]. Saidane E. H, D. Scida, M. Assarar, H. Sabhi and R. Ayad (2016). "Hybridisation effect on diffusion kinetic and tensile mechanical behaviour of epoxy based flax–glass composites." Composites Part A: Applied Science and Manufacturing 87: 153-160.

5]. Keller Michael W, Jellison B. D, Ellison T. (2013). Moisture effects on the thermal and creep performance of carbon fiber/epoxy composite for structural pipelines repair. *Elsevier Ltd*, 45, 1173-1180.

6]. Kim H-Y, Y-H. Park, Y-J You and C-K. Moon (2008)."Short-term durability test for GFRP rods under various environmental conditions." Composite Structures 83(1):37-47.

7]. Guedes, R. M, Sá A, and Faria H. (2007). "Influence of moisture absorption on creep of GRP composite pipes." Polymer Testing 26(5): 595-605.

8]. Greentech, G. (2016) "FRP Pressure Pipe". Retrieved from www.gilgwang.co.kr.

9]. Langhelle, M. B. (2011). *Pipelines for Development at Deep Water Fields.* University of Stavanger, Faculty of Science and Technology. Offshore Technology/ Marine and Subsea Technology, Master Thesis.

10]. Davies P, Boisseau A, Choqueuse D, Peters L, Renaud C, Nickel R, Thiebaud F, Perreux D, (2010). Marine Composite for Ocean energy Application: Ensuring long-term durability. *Third International Conference on Ocean Energy.*

11]. Pavlov D. G, (2013) Composite Materials in Piping Application: Design, Analysis and Optimization of Subsea and Onshore Pipelines from FRP Composites. DEStech Publication, ISBN No. 978-1-60595-029-7

12]. Martin R, (The Institute of Materials, Minerals & Mining, 2008) The Aging of Composites, Woodhead Publishing and Maney Publishing.

13]. Baker A, Dutton S, and Kelly D, (2004). *Composite Materials for Aircraft Structure* (Second Edition ed.). American Institute of Aeronautics and Astronautics, Inc.

14]. Hawa A, Abdul Majid M. S, Afendi M, Marzuki H. F. A, Amin N. A. M, Mat F. and Gibson A. G. (2016). "Burst strength and impact behaviour of hydrothermally aged glass fiber/epoxy composite pipes." Materials & Design 89: 455-464.

15]. Onder A, Sayman O, Dogan T, and Tarakcioglu N. (2009). "Burst failure load of composite pressure vessels." Composite Structures 89(1): 159-166.

16]. Abdul Majid M. S, Afendi M, Afendi P, M. Haslan, Krishnan P, Amin A. M, (2014). Ageing effects on burst pressure test of impacted glass fibre reinforcement epoxy (GRE) pipes. *Trans Tech Publications, Switzerland, 695*, 717-720.

17]. D3039/D3039M-00, ASTM. (2000). *Standard Test Method for Tensile Properties of Polymer Matrix Composite Materials.* ASTM International.

18]. D790-02, ASTM. (2002). *Standard Test Method for Flexural Properties of Unreinforced and Reinforced Plastics Electrical Insulating Materials.* ASTM International.

19]. D2990-01, ASTM. (2001). *Standard Test Method for Tensile, Compressive, and Flexural Creep and Creep-Rupture of Plastics.* ASTM International.

20]. Guo B, Song S, Ghalambor A, and Lin T, (2014). *Offshore Pipelines (Design, Installation and Mantenance) Second Edition.* Elsevier Inc.

21]. Krishnan P, M. S. Abdul Majid, M. Afendi, A. G. Gibson and H. F. A. Marzuki (2015). "Effects of winding angle on the behaviour of glass/epoxy pipes under multiaxial cyclic loading." Materials & Design 88: 196-206.
22]. D1598-02, ASTM. (2002). *Standard Test Method for Time-to-Failure of Plastic Pipe Under Constant Internal Pressure.* ASTM International.
23]. D1599-99, ASTM. (2000). *Standard Test Method for Resistance to Short-time Hydraulic Pressure of Plastic Pipe, Tubing, and Fitting.* ASTM International.
24]. D3517-04, ASTM. (2004). *Standard Specification for "Fiberglass" (Glass-Fiber-Reinforced Thermosetting-Resin) Pressure Pipe.* ASTM International.
25]. D638-08, ASTM. (2008). *Standard Test Method for Tensile Properties of Plastics.* ASTM International.
26]. Mallick P. K. (2007). *Fiber-Reinforced Composite (Materials, Manufacturing, and Design) Third Edition.* Taylor and Francis Group, LLC.
27]. Hearn, E. J. (1997). *Mechanics of Materials 2* (Third Edition ed.). Butterworth Heinemann.
28]. D2992-01, ASTM. (2001). *Standard Practice for Obtaining Hydrostatic or Pressure Design Basis for "Fiberglass" (Glass-Fiber-Reinforced Thermosetting-Resin) Pipe and Fitting.* ASTM International.
29]. Na L, Sirong Z, Jianzhong C, Xi F. (2015). Long-term behavior of GFRP pipes: Optimizing the distribution of failure points during testing. *Elsevier Ltd*, 48, 7-11.
30]. Faria H, Guedes R. M. (2010). Long-term behaviour of GFRP pipes: Reducing the prediction test duration. *Elsevier Ltd*, 29, 337-345.
31]. Rafiee R. (2016). "On the mechanical performance of glass-fiber-reinforced thermosetting-resin pipes: A review." Composite Structures 143: 151-164.
32]. Arikan H. (2010). "Failure analysis of ($\pm$55°) filament wound composite pipes with an inclined surface crack under static internal pressure." Composite Structures 92(1): 182-187.
33]. Gemi L, Tarakçioğlu N, Akdemir A. and Şahin Ö. S. (2009). "Progressive fatigue failure behavior of glass/epoxy ($\pm$75)"Filament-wound pipes under pure internal pressure." Materials & Design 30(10): 4293-4298.
34]. Banakar P, Shivananda H. K, and Niranjan H. B. (2012). Influence of fiber orientation and thickness on tensile properties of laminated polymer composites. *International Journal of Pure and Applied Science and Technology, 9(1)*, 61-68.
35]. Gibson A. G, Ortheguy Torres M. E, Browne T.N.A, Feih S, and Mouritz A.P, (2010). High temperature and fire behaviour of continuous glass fibre/polypropylene laminates. *Composite: Part A, 41*, 1219-1231.
36]. Chevali, V. S, Dean D. R. and Janowski G. M. (2009). "Flexural creep behavior of discontinuous thermoplastic composites: Non-linear viscoelastic modeling and time–temperature–stress superposition." Composites Part A: Applied Science and Manufacturing 40(6-7): 870-877.
37]. Enamul H. M. (2011). "The current and future trends of composite materials: an experimental study." Journal of Composite Materials 45(20): 2133-2144.
38]. Deniz M. E, Ozdemir O, Ozen M, and Karakuzu R. (2013). Failure pressure and impact response of glass'epoxy pipes exposed to seawater. *Elsevier, Ltd, 53*, 355-361.
39]. McKeen, L. W. (2015). "Introduction to Creep, Polymers, Plastics and Elastomers." 1-41.
40]. T. Shaw Montgomery, MacKnight W. J. (2005). *Introduction to polymer viscoelasticity.* Wiley Interscience.

41]. Ngan A. H. W, Smallman R. E. (2014). *Modern Physical Metallurgy* (Eighth Edition ed.). Elsevier Ltd.
42]. Roylance, D. (2008). *Mechanical Properties of Materials* . MIT Publisher.

4. Results and Discussion

4.1 Short-term test

4.1.1 Burst Pressure Test of FRP Composite Pipes

The maximum internal pressure and time dependent internal pressure results were not obtained, due to the fact that the experimental setup of FRP composite pipes of HFW ±45° and HFW ±55° was not possible to use. There were several disturbances that occurred during experimental of burst pressure test, such as:

a). Fastening of aluminum lid disc to the FRP composite pipes at outer diameter of FRP composite pipe were unprecise enough. Therefore, fastening bolts distance position were not in similar position to fix the FRP composite pipe where the aluminum grip slip along the steel grips from the fastening bolts.

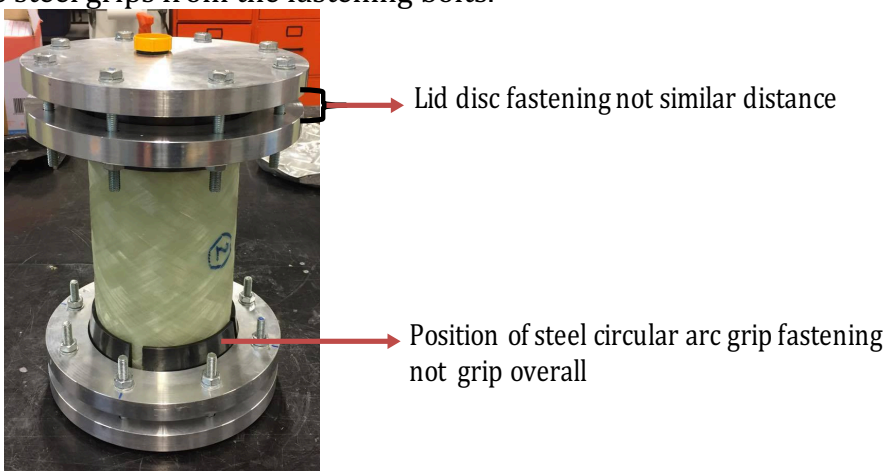

Figure 17. FRP composite pipes experimental setup

b). Oval shape of inner and outer diameter FRP composite of HFW, hence seals are not in good sealing conditions from the hydrostatic internal pressure of HFW FRP composite pipes under internal pressure testing.

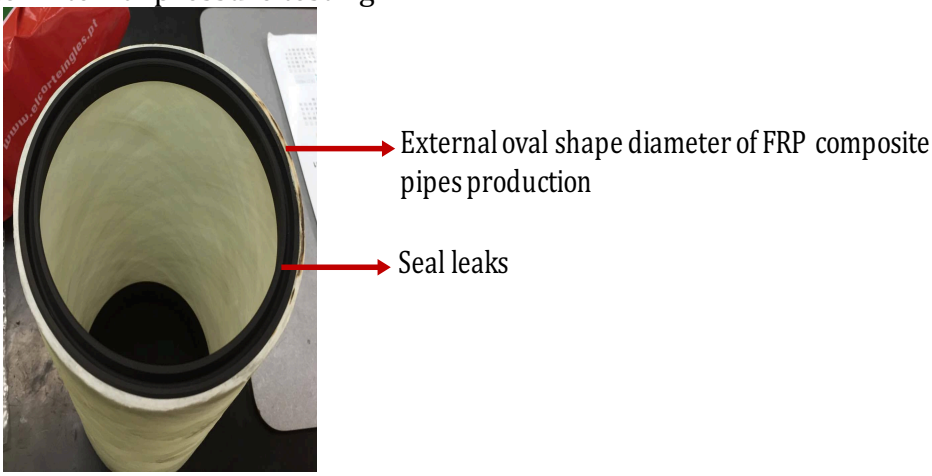

Figure 18. Seal for inner tube of FRP composite pipe

c). The steel grip contact from outer surface of FRP composite pipes is unprecise to the oval shape of outer diameter FRP composite pipes and when over fastening from the fastening bolts for internal hydrostatic pressure occurred crack propagation of FRP composite pipes tube wall occurred. Therefore, FRP composite pipes were not able to obtain internal pressure data from the experimental tests. Meanwhile, when hydrostatic

pressure increases, air and water pressure leaks through the crack propagation of FRP composite pipe [1-8].

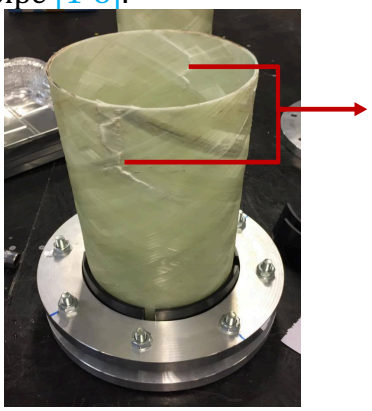

Figure 19. Crack propagation from FRP composite setup

4.1.2 Tensile Test of FRP Composite Pipes

Experimental testing of FRP composite pipe specimens was done using an universal testing machine with velocity 2 mm/min for unconditioned specimens and ageing conditioned specimens at varying immersions; water immersion, WI, sea water immersion, SWI, and diesel immersion, DI, at ambient temperature and water immersion, WI, at 60 ˚C. The results are shown in figure 20 part (1) and part (2) for the maximum stress and maximum strain [9]. For the specimens testing with HFW ±45° and thickness 3,33 mm, the maximum stress and maximum strain at ambient temperature, shown in figure 20 part (1), the DI specimen, P7D45TT, maximum stress is considered as the highest tensile stress at 17,048 MPa and followed by WI specimens, P12W45TT, tensile stress at 16,054 MPa. SWI specimen, P6SWI45TT and unconditioned specimens P3V45TT tensile stress are approximately same at 15 MPa.

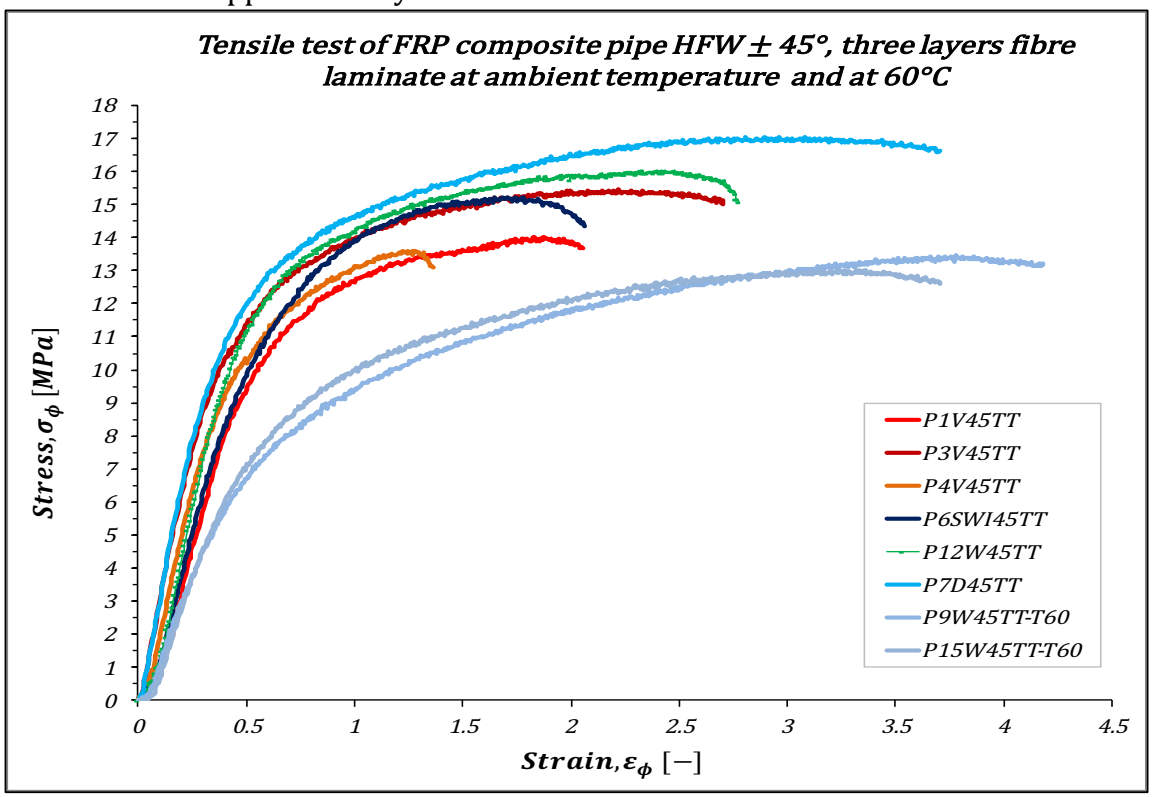

(1)

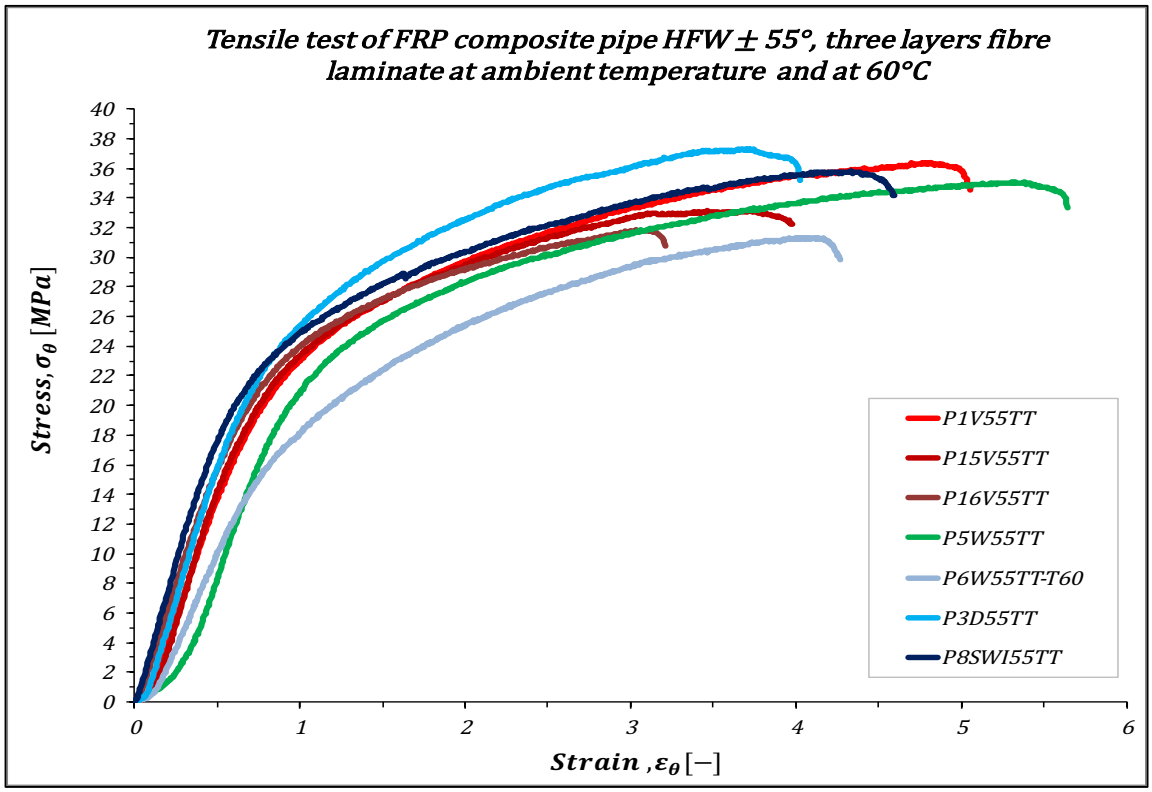

(2)

Figure 20. FRP HFW ±45° and HFW ±55° composite pipes tensile test results

The HFW of FRP composite pipe in WI specimens P9W45TT-T60 and P15W45TT-T60 at 60°C show that the FRP composite pipe stress properties are very low in contrast to the FRP composite pipe in unconditioned specimens P1V45TT and P4V45TT of FRP composite pipe [10].

The FRP composite pipe tensile test of HFW ±55° as shown in figure 20 part (2) unconditioned and different ageing conditioned in WI, SWI, DI at ambient temperature and WI at 60°C show that the HFW of FRP composite pipe DI specimen, P3D55TT, has relative higher tensile stress at 37,307 MPa, followed by sea water specimen, P8SWI55TT, at tensile stress 35,793 MPa. The HFW ±55° of FRP composite pipe with conditioned in WI specimen, P6W55TT-T60, at 60°C is considered with the lowest stress properties. In figure 21 part (1), it is shown that for the HFW ±45° of FRP composite pipe the maximum force of the experimental and maximum force analysis are approximately the same for unconditioned specimens P1V45TT, P3V45TT and P4V45TT and conditioned in WI specimens P9W45TT-T60 and P15W45TT-T60 at 60°C. The others WI specimen, P12W45TT, DI specimen P7D45TT and SWI specimen, P6SWI45TT are relatively the same for experimental tensile force of FRP composite pipe HFW ±45° specimens test. The FRP composite pipe DI specimen, P7D45TT, considered as higher maximum force is 1334,119 N in tensile test. The HFW ±55° of FRP composite pipe shown in figure 21 part (2) states that the FRP composite pipe in DI specimen, P3D55TT high tensile force is 3727,046 N. Meanwhile, the FRP composite pipe WI specimen, P6W55TT-T60 at 60°C has the lowest tensile force in experimental test.

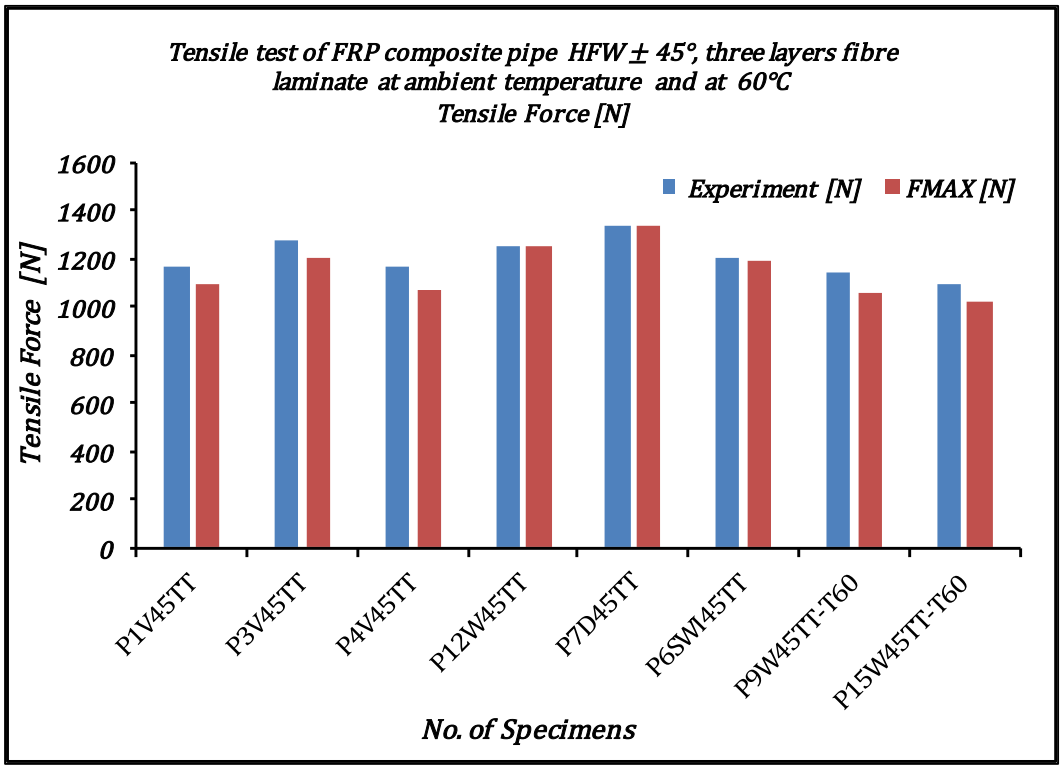

(1)

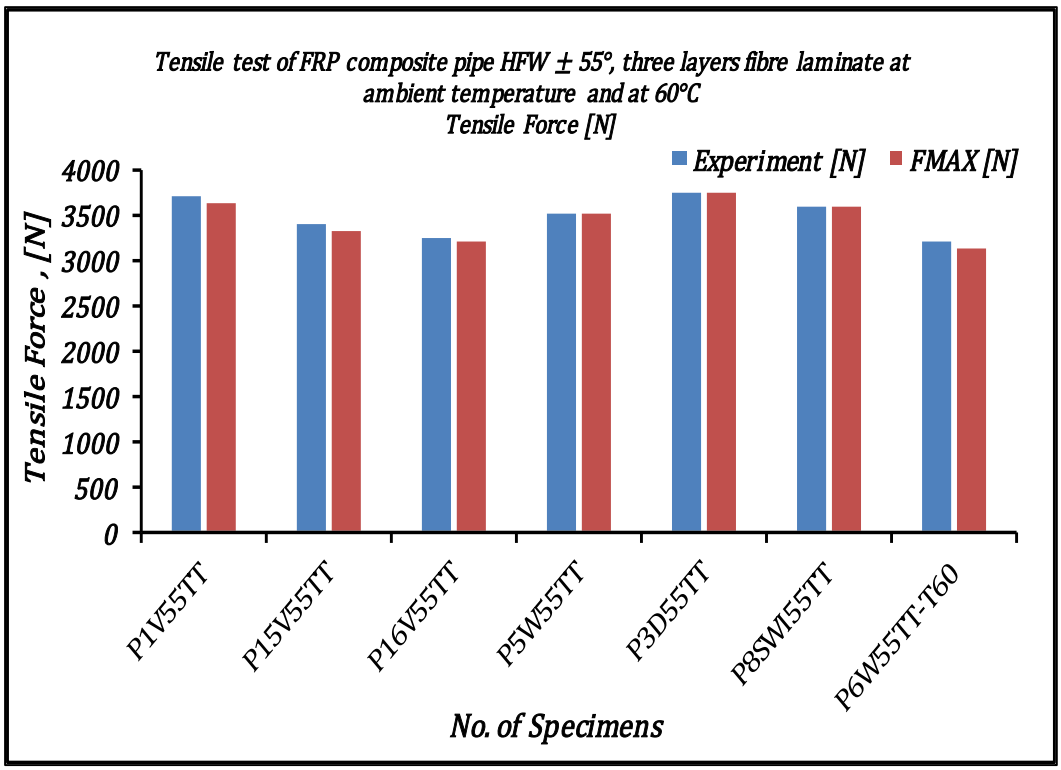

(2)

Figure 21. Tensile force FRP HFW ±45° and HFW ±55° of composite pipes

For the different ageing of FRP HFW composite pipe specimens, unconditioned and conditioned in different method of WI, SWI, DI at ambient temperature and WI at 60°C, the existence of error data in the experiments are dependent on specimens. The error

data occurrences affected to the maximum stress and maximum strain that could change the properties from data acquisitions of FRP composite pipe.

Tensile test of FRP composite pipe HFW ± 45°, three layers fibre laminate at ambient temperature and at 60°C		
Percentange of Error Occurrence in Experimental Data		
Specimens	*Error Points*	
P1V45TT	*5,97*	*%*
P3V45TT	*3,70*	*%*
P4V45TT	*11,17*	*%*
P12W45TT	*3,85*	*%*
P7D45TT	*2,08*	*%*
P6SWI45TT	*2,49*	*%*
P9W45TT-T60	*6,10*	*%*
P15W45TT-T60	*4,16*	*%*

(1)

Tensile test of FRP composite pipe HFW ± 55°, three layers fibre laminate at ambient temperature and at 60°C		
Percentange of Error Occurrence in Experimental Data		
Specimens	*Error points*	
P1V55TT	*2,49*	*%*
P15V55TT	*1,12*	*%*
P16V55TT	*3,63*	*%*
P5W55TT	*3,38*	*%*
P3D55TT	*0,56*	*%*
P8SWI55TT	*2,84*	*%*
P6W55TT-T60	*5,10*	*%*

(2)

Table 6. The error occurred in tensile test of HFW ±45° and HFW ±55°

The table 6 in part (1) and part (2) show the existence of error FRP HFW of composite pipe in different HFW ±45° and HFW ±55° as from initial point, middle point and end. It can be considered that with unconditioned specimen P4V45TT at ambient temperature has occurred the highest error and DI specimen P7D45TT has the smallest error occurred for HFW ±45° at the initial points. Considering the error occurred in HFW ±55° of FRP composite pipe, WI specimen P2W55TT-T60 has the highest errors followed by the WI specimen P6W55TT-T60 and DI specimen P3D55TT is considered as smallest error occurred at initial points for tensile test specimens. More deeply, for overall specimens data acquisition in the experiment, if the errors data is increasing, the engineering stress and engineering strain data becomes small or decrease.

The experimental error data occurrence defined as:

Percentage of error occurrence in experimental data, $E_{error}[\%]$

Number of error data at initial point, middle point and ended point, $N_{IP,MP,EP}$

Overall experimental data acquisition, n.

$$E_{error}[\%] = \frac{N_{IP,MP,EP}}{n} * 100$$

The rupture types of HFW ±45° and HFW ±55° FRP composite pipe for unconditioned and conditioned at ambient temperature and at 60°C are starting from whitening colors of specimens when at higher stress load the whitening colors appears randomly on surface of the specimens of FRP composite pipe as indicated in the figure 22 part (1) and part (2) for HFW ±45° and HFW ±55° [11-17].

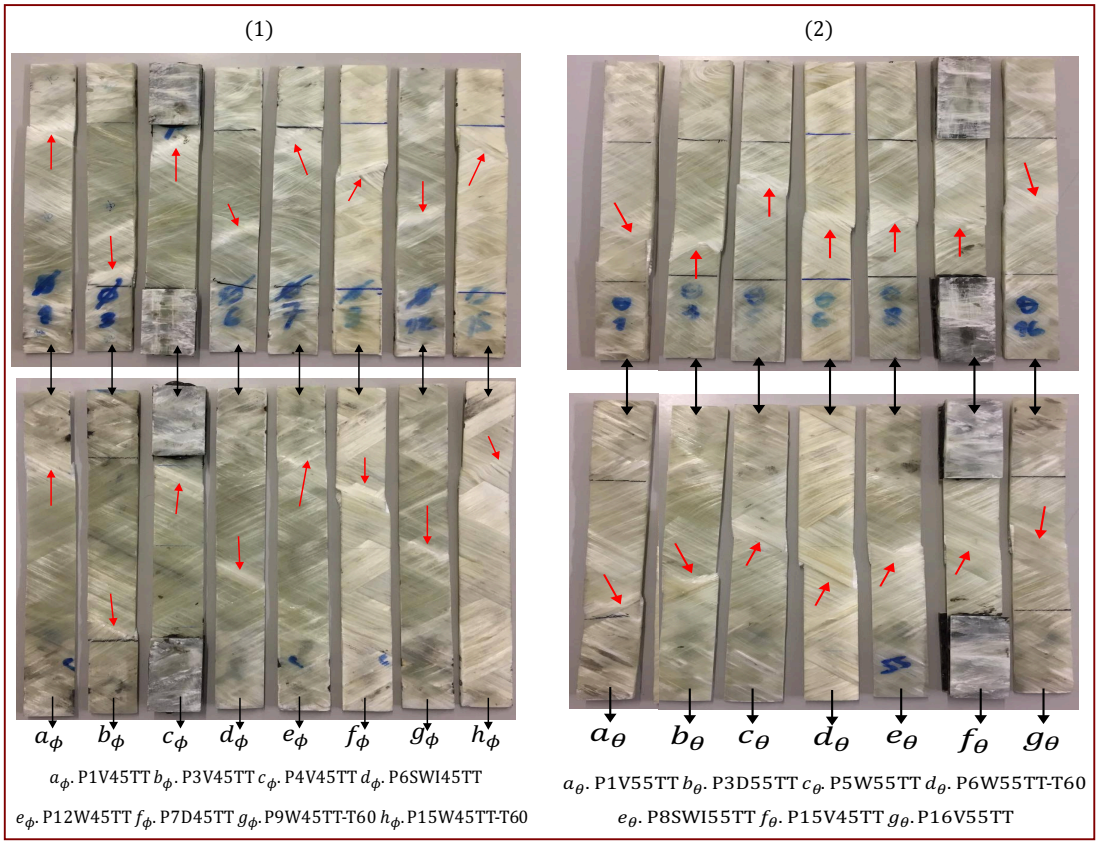

Figure 22. Rupture type of HFW ±45° and HFW ±55° composite pipes

The rupture types of HFW ±45° are short cross breaks propagation at fibre and matrix surface to the fibre direction and the break type of HFW ±55° show long cross breaks propagation at fibre and matrix surface to the fibre direction.

Meanwhile, for the HFW ±45° and HFW ±55° of FRP composite pipe at 60°C, when, at the maximum tensile stress, perform the large short cross breaks of fibre and matrix are peeling then pull out from the surface of the HFW ±45°. When strain is increasing and at surface of fibre and matrix are also peeling initially and then pulled out by large cross breaks and long propagation at fibre and matrix surface to the fibre direction of HFW ±55° [17].

4.1.3 Three-Point Bending Creep Test of FRP Composite Pipes

Time dependent three-point bending creep test of HFW ±45° and HFW ±55° FRP composite pipes are realized by bending test at constant loading. The constant load is converted to the mass of the free leg cantilever bar that is fixed to the rotation bearing

where pushes the stainless-steel rod contact to the circular arc beam of FRP composite pipe. The linear variable displacement transducer (LVDT) is moving simultaneously with the stainless-steel rod during 10080 minutes or less, depending upon maximum deep FRP composite circular arc beam deflection $d_y \leq 24$ mm [18,19]. Two different HFW ±45° and HFW ±55° three-point bending experiments were conducted for unconditioned and conditioned in different ageing: WI, SWI and DI at ambient temperature and WI at 60°C.

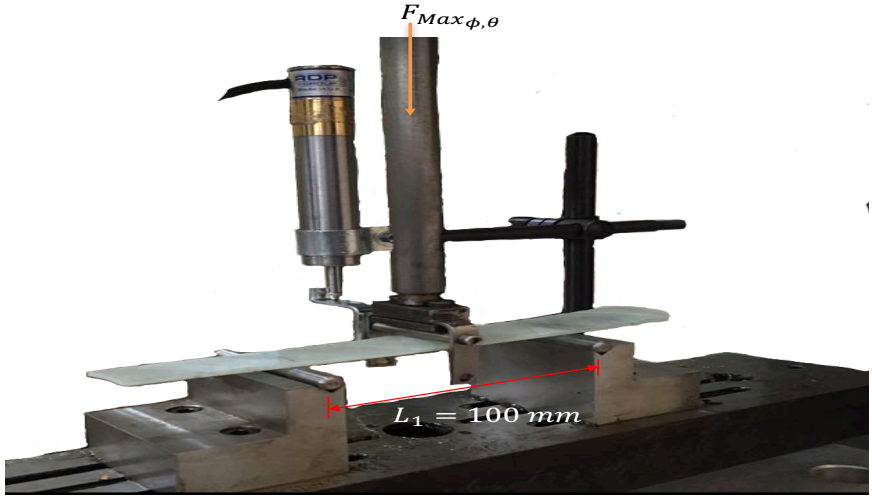

Figure 23. Three-point bending FRP of circular arc beam geometry

The time dependent strain of FRP composite pipe HFW ±45° of circular arc beam at stress level configuration $\sigma_\phi = 0{,}258$ MPa [1,8%] with thickness geometry $t_\phi = 3{,}33$ mm and HFW of circular arc beam at stress level configuration ±55° $\sigma_\theta = 0{,}338$ MPa [1%], $\sigma_\theta = 0{,}473$ MPa [1,4%] and $\sigma_\theta = 0{,}338$ MPa [1,8%] with $t_\theta = 4{,}24$ mm are expressed graphically.

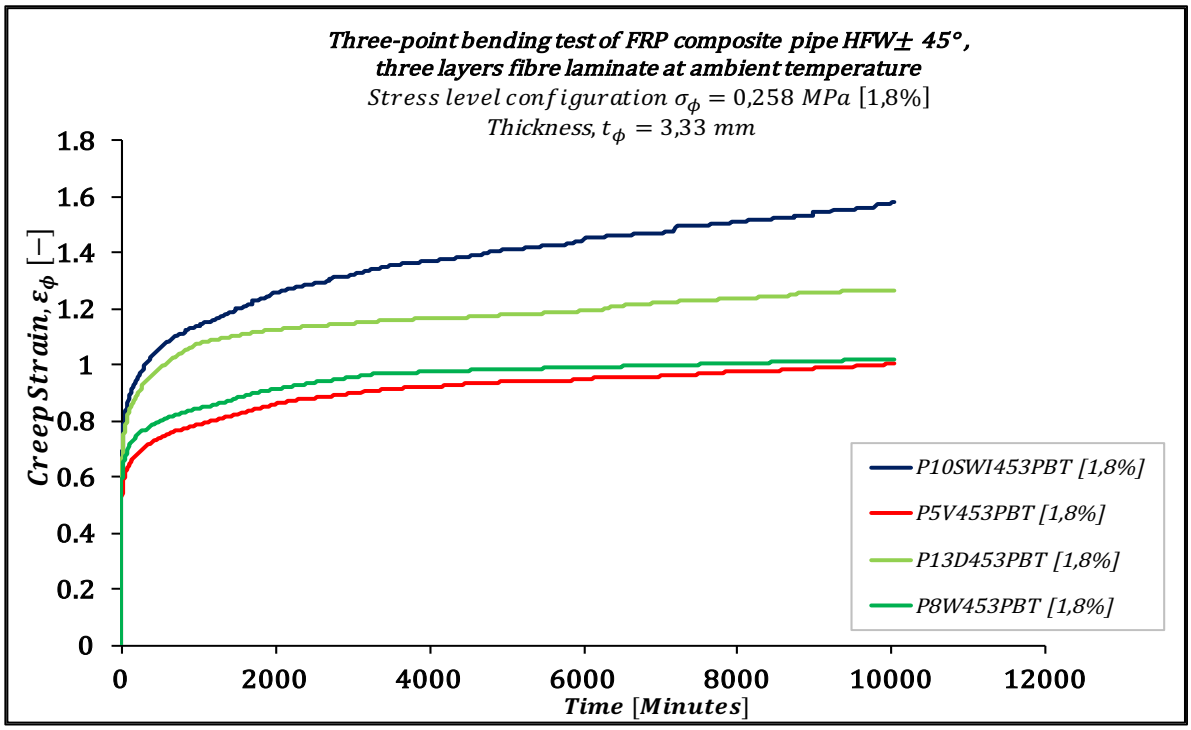

Figure 24. Creep strain of HFW ±45° FRP composite pipes

Circular arc beam specimen of FRP composite pipe HFW ±45° with thickness, t_ϕ = 3,33 mm, at ambient temperature and the stress level configuration 0,258 MPa [1,8%] show that unconditioned specimen, P5V453PBT and water immersion specimens P8W453PBT, WI, have approximately small strain whilst the diesel immersion P13D453PBT, DI, and sea water immersion P10SWI453PBT, SWI, are approximately similar at instantaneous stress, then sea water immersion P10SWI453PBT strain increased extremely and having higher creep strain than petrol immersion P13D453PBT. The strain level of unconditioned specimen P5V453PBT and WI, P8W453PBT conditioned show nonlinear viscoelastic strain. However, the viscoelastic strain starting from the beginning and for the unconditioned P5V453PBT and WI conditioned P8W453PBT specimens are show fluctuation nonlinear creep strain. The FRP circular arc beam specimen conditioned in DI shows nonlinear viscoelastic strain is very high in comparison to the unconditioned and WI specimens P8W453PBT viscoelastic strain level. The SWI specimen P10SWI453PBT viscoelastic strain are considered as very low strain level in comparison to the unconditioned specimen and for WI specimen P8W453PBT the strain level is linear viscoelastic extremely very high at time dependent of strain.

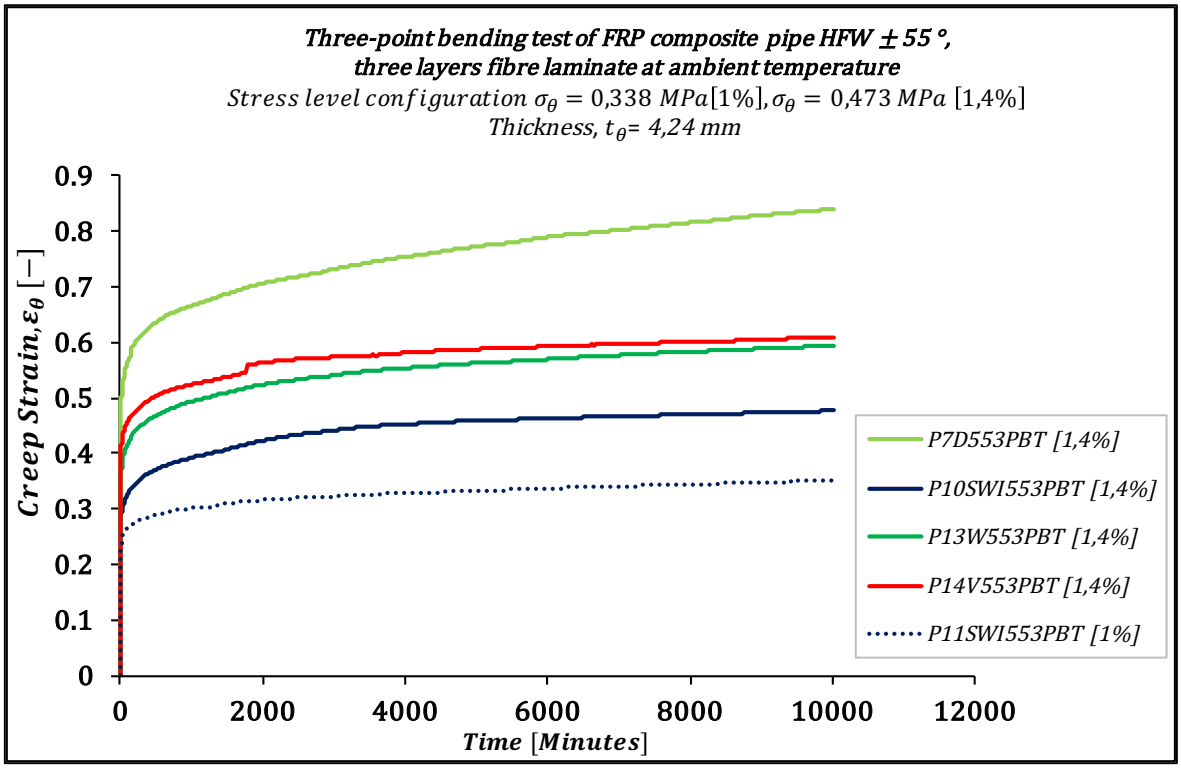

Figure 25. Creep strain of HFW ±55° FRP composite pipes

The results of circular arc beam specimen of FRP composite pipe of helicoidal filament winding, HFW ±55° with thickness, t_θ = 4,24 mm, at ambient temperature and at the stress level σ_θ = 0,338 MPa [1%], σ_θ = 0,473 MPa [1,4%] are shown in figure 25 and σ_θ = 0,258 MPa [1,8%] is shown in figure 26. It can be seen that in SWI specimen, P11SWI553PBT strain at stress level σ_θ = 0,338 MPa [1%] has occurred small viscoelastic strain and perform the nonlinear time dependency in 10080 minutes. At the

stress level, $\sigma_\theta = 0{,}473$ MPa [1,4%], it is shown that with SWI specimen P10SWI553PBT has occurred small strain, whilst WI specimen P13W553PBT and unconditioned specimen P14V553PBT have higher strain and very similar viscoelastic in 10080 minutes and perform nonlinear viscoelastic strain. In the DI specimen P7D553PBT has occurred very high viscoelastic strain and perform small linear viscoelastic strain in 10080 minutes. DI specimen P7D553PBT viscoelastic strain approximately increase two times than SWI specimen, P10SWI553PBT. FRP composite pipe circular arc SWI specimen P4SWI553PBT at stress level $\sigma_\theta = 0{,}258$ MPa [1,8%] has shown that the viscoelastic strain is extremely high and within a short time at 202 minutes the time dependent strain approach the maximum strain. The viscoelastic strain performs small fluctuation within the linear viscoelastic. Furthermore, SWI specimens, P11SWI553PBT [1%], P10SWI553PBT [1,4%] (in figure 25) and P4SWI553PBT [1,8%] (in figure 26) at three different stress level configurations 1%, 1,4% and 1,8% of helicoidal filament winding ±55° perform different viscoelastic strain and if the stress level is small, the viscoelastic strain occurred proportionally small to the stress level configuration.

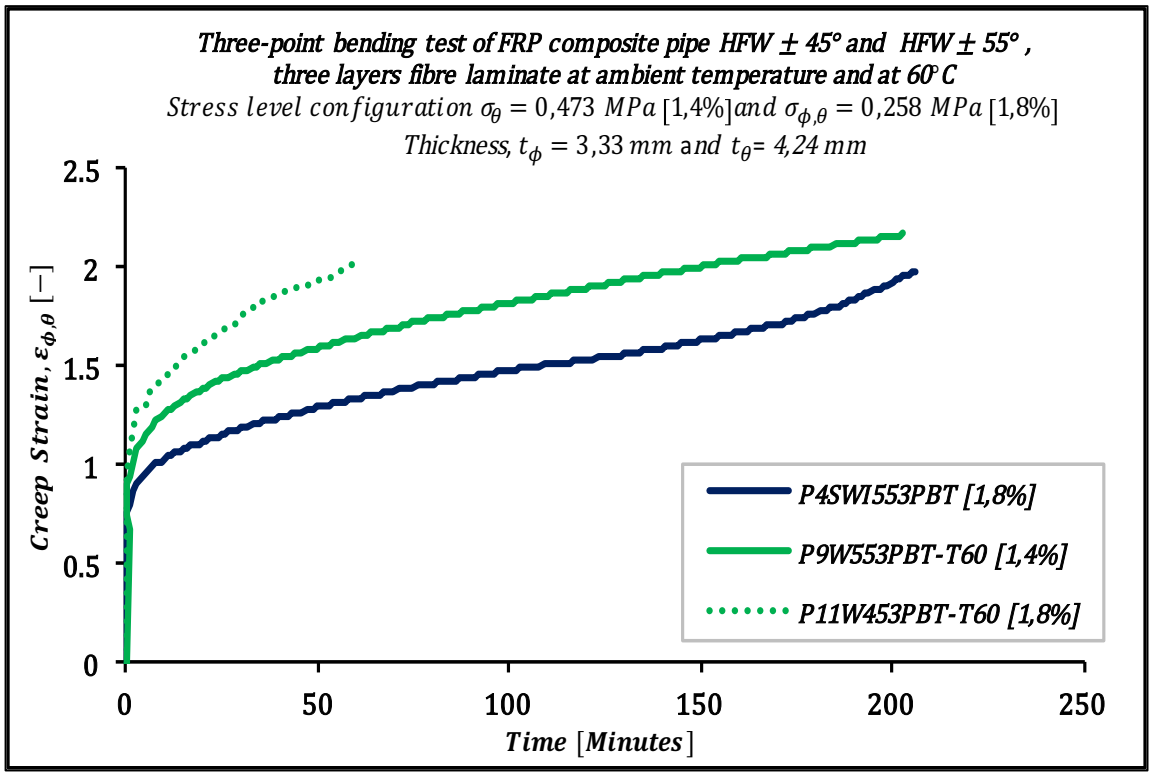

Figure 26. Creep strain of HFW ±45° and HFW ±55° FRP composite pipes

Regarding FRP composite pipe specimen at 60°C in water immersion, WI, the tests were conducted for two different stress level configurations of two different helicoidal filament winding, HFW ±45° and HFW ±55°. For HFW ±45° performed at stress level configuration 1,8% and for HFW ±55° at stress level 1,4% results are shown in figure 26. Circular arc beam specimen of HFW ±45° in WI, P11W453PBT-T60 at 60°C obtained the viscoelastic time dependent strain extremely quick, hence, within 70 minutes approached the maximum viscoelastic strain. Circular arc beam specimen of HFW ±55° WI,

P9W553PBT-T60 at 60°C performed the viscoelastic strain extremely with high velocity creep deflection. The three-point bending creep test deformation was reached in 212 minutes and the experimental has shown that increase linearly.

Creep compliance of three-point bending test of FRP composite pipes is defined as the time dependent strain per unit stress of HFW ±45° and HFW ±55° of FRP composite pipes. The creep compliance of HFW ±45° of circular arc beam at stress level configuration 0,258 MPa [1,8%] is shown in figure 27. Considering that if the fibre laminate HFW direction is very nearly to 90° the stiffness of FRP composite pipe design will be very small for bending applications.

Therefore, as shown in the figure 27, the FRP composite pipe circular arc beam SWI specimen, P10SWI453PBT, show the specimen is most critical creep compliance under constant loading stress level 1,8%. The stiffness of SWI specimen, P10SWI3PBT gradually decreased by large linear viscoelastic time dependent strain within 10080 minutes.

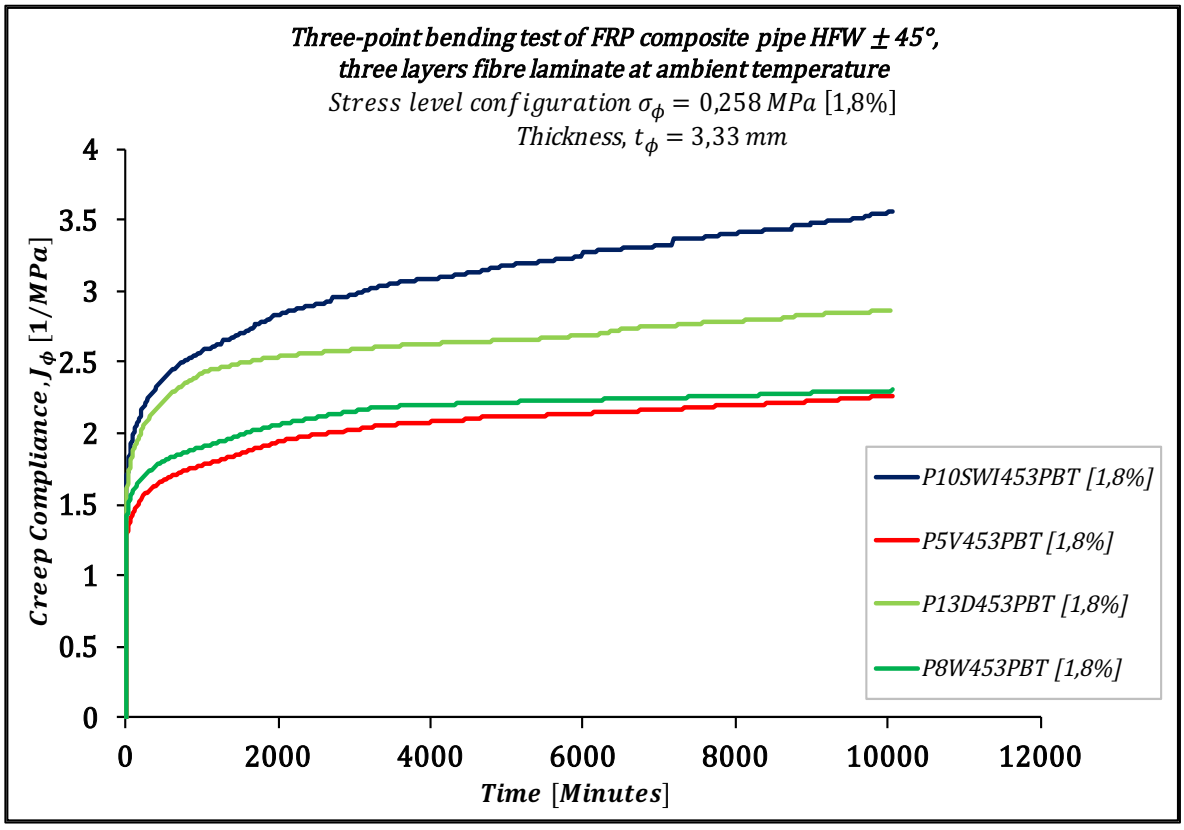

Figure 27. Creep compliance of HFW ±45° FRP composite pipes

Unconditioned specimen, P5V453PBT and WI specimen, P8W453PBT are performing similar creep compliance nonlinearity model and the difference is the creep compliance level of unconditioned specimen, P5V453PBT, relatively higher than WI specimen, P8W453PBT. Therefore, the viscoelastic deformation of unconditioned specimen, P5V453PBT has highest creep compliance than the WI specimen P8W453PBT, DI specimen, P13D453PBT and SWI specimens, P10SWI453PBT of HFW ±45°. More explanation, HFW ±45° 1,8% stress level configuration unconditioned, P5V453PBT, and conditioned in WI specimen, P8W453PBT, DI specimen P13D453PBT and SWI specimen

P10SWI453PBT for offshore and onshore industries applications, remain high strength of creep compliance, however occurred variant adequate strain viscoelastic deformation [20-23].

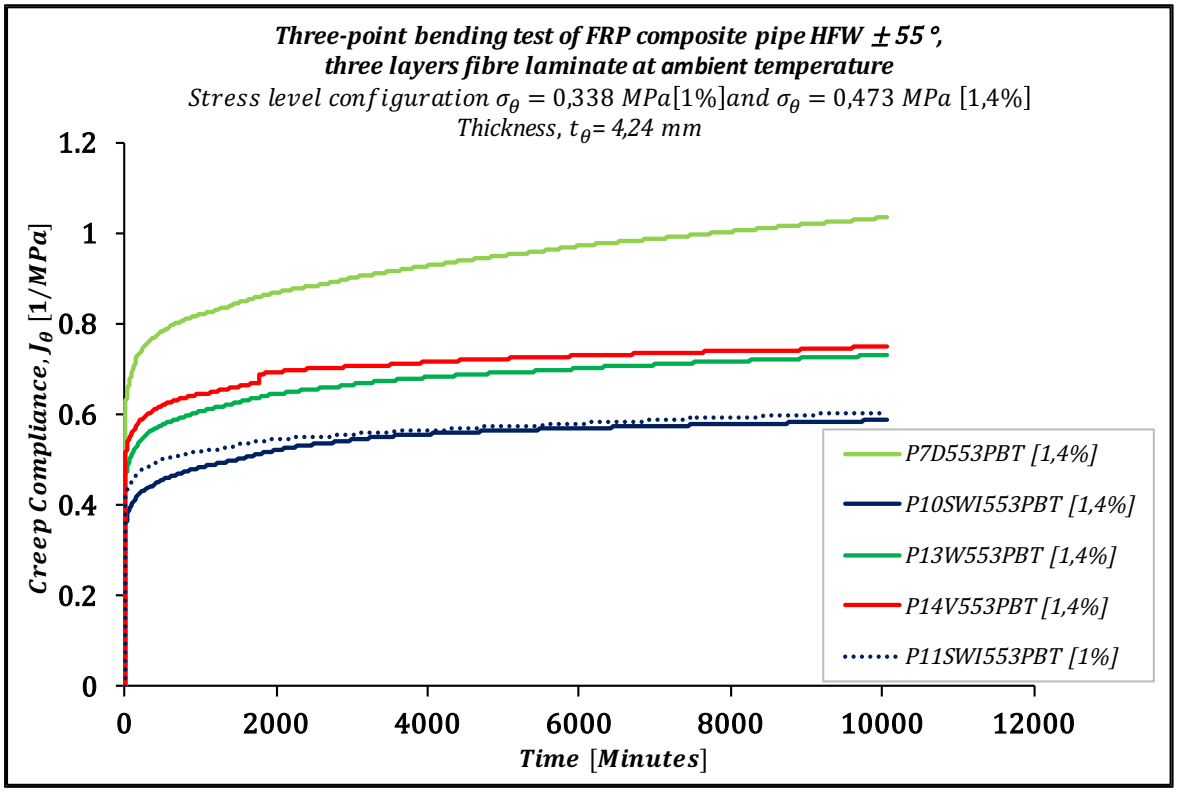

Figure 28. Creep compliance of HFW ±55° FRP composite pipes

In figure 28, it is shown the creep compliance of three-point bending test FRP composite pipes of HFW ±55° at the stress levels configuration 1%, 1,4% and 1,8%. Overall specimens, the experiment shows remarkable creep compliance properties, even performing at different ageing conditioned and unconditioned showing different nonlinearity at viscoelastic deformation.

More specific explanation, the FRP composite pipe conditioned in SWI specimen, P11SWI553PBT [1%] and P10SWI553PBT [1,4%] for different stress levels and HFW ±55°, the creep compliance for viscoelastic strain is approximately the same even if the specimen is in high moisture absorption of sea water salinity. However, the property show that the creep compliance at stress level configuration 1% and 1,4% of SWI specimens P11SWI553PBT [1%] and P10SWI553PBT [1,4%] are considerably high than unconditioned specimen and conditions in WI specimen, P13W553PBT and DI specimen P7D553PBT whilst, if the stress level increases more to 1,8%, as shown in figure 29 for specimen P4SWI553PBT, the creep compliance presents extremely low value. When deflection increase with time the creep compliance extremely show small linear deformation, therefore under the short time viscoelastic deformation of the specimen approached the maximum deflection.

The percentage of undamaged deformation is not considerable in comparison with the unconditioned specimen, P14V553PBT and conditioned in WI specimen, P13W553PBT

DI specimen, P7D553PBT and SWI specimen, P10SWI553PBT of HFW ±55° at stress level configuration 1,4%.

The creep compliances of FRP composite pipe for high temperature application as chemical industries, are shown in the figure 29. The HFW ±45° and HFW ±55° of FRP composite pipe at high temperature application perform the fibre and matrix to water absorption at 60°C and stress level 1,8% for HFW ±45°and stress level 1,4% for HFW ±55° to the three-point bending creep test at constant stress loading, individually HFW ±45° 1,8% specimen shows extremely low creep compliance.

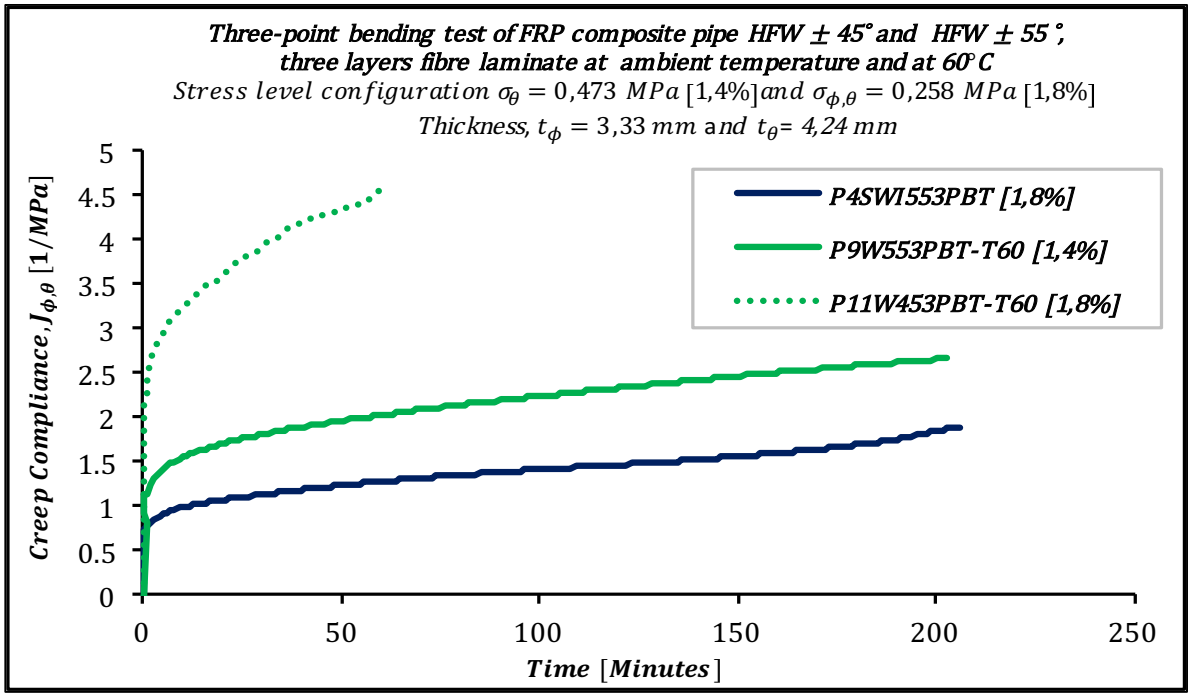

Figure 29. Creep compliance of HFW ±45° and HFW ±55° FRP composite pipes

The FRP composite pipe creep compliance of WI specimen, P11W453PBT-T60 under the 70 minutes approached to the maximum deformation. So, this is considering fibre laminate and matrix at helicoidal filament winding ±45°, the degradation to the temperature absorption at viscoelastic strain easily damaged by the high linear deformation.

For the HFW ±55° 1,4% at stress level configuration and at 60°C, occurred extremely low viscoelastic strain during 10080 minutes. As shown in figure 29, the FRP composite pipe specimen, P9W553PBT-T60, approached linear large deformation within the 212 minutes.

From the experimental results of HFW ±45°and HFW ±55° of three-point bending creep test, these properties could be identified by the fibre direction in helicoidal filament winding production of FRP composite pipe explain as if helicoidal filament winding of FRP composite approximately increase closed to the angle 90°, the creep compliance of FRP composite pipe increases extremely from constant loading of three-point bending creep test.

The regression analysis of FRP composite pipes HFW ±45° and HFW ±55° from the experimental analysis result will not evaluate overall for failure time prediction. Due to the several experimental results of FRP composite pipes HFW ±45° and HFW ±55°, the creep strain and creep compliance are not required for failure lifetime prediction [24-27]. The experimental regression analysis that are not recommendable for failure lifetime prediction FRP composite pipes HFW ±45° is water immersion specimen, WI, at 60˚C P11W453PBT-T60 at stress level configuration $\sigma_\theta = 0{,}258\ MPa$ [1,8%]. For the HFW ±55° FRP composite pipes, water immersion specimen, WI, at 60˚C, P9WI553PBT-T60 at stress level $\sigma_\theta = 0{,}473\ MPa$ [1,4%] and sea water immersion specimen, SWI, P4SWI553PBT at stress level $\sigma_\theta = 0{,}258\ MPa$ [1,8%] are also not recommendable for failure lifetime prediction.

Optimization of statistical distribution of the test log-log regression model of the short-term test property prediction of viscoelastic properties for FRP composite pipe circular arc beam under 10080 minutes are will carried out on 1000 hours [19]. The logarithmic data analysis of FRP composite pipes HFW ±45° and HFW ±55° are defined by logarithm base scale 10. Strain of FRP composite pipe vs failure lifetime data regression analysis for HFW ±45° performed as:

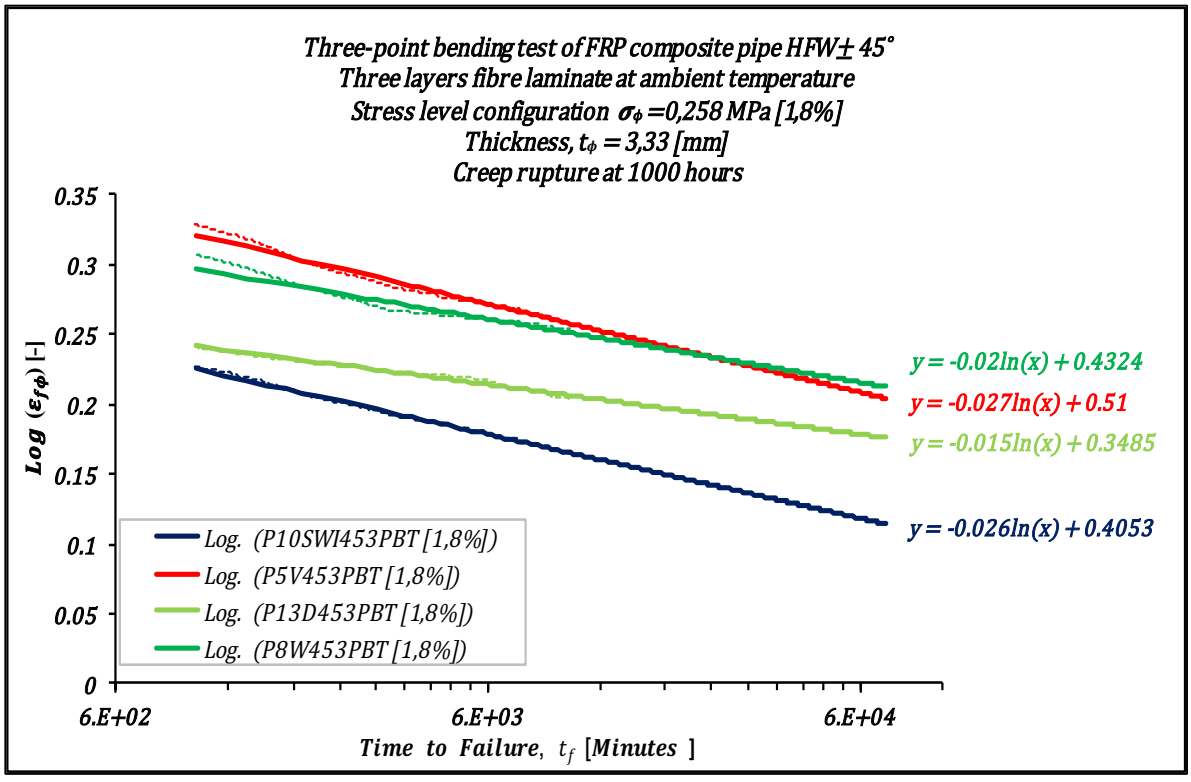

Figure 30. Failure lifetime prediction of FRP composite pipes HFW ±45° at 1000 hours

Unconditioned specimen, P5V453PBT logarithmic regression analysis model

$$1000\text{h}\ \log(\varepsilon_f) = 0{,}51 - 0{,}027\ \log(t_u)$$

Seawater immerse, SWI specimen P10SWI453PBT logarithmic regression analysis model

$$1000\text{h}\ \log(\varepsilon_f) = 0{,}4053 - 0{,}022\ \log(t_u)$$

Water immerse, WI specimen P8W453PBT logarithmic regression analysis model

$$1000\text{h}\log(\varepsilon_f) = 0{,}4324 - 0{,}021\log(t_u)$$

Diesel immerse, DI specimen P13D453PBT logarithmic regression analysis model

$$1000\text{h}\log(\varepsilon_f) = 0{,}3485 - 0{,}015\log(t_u)$$

The failure lifetime for HFW $\pm 45°$ at 1000 hours under stress level configuration $\sigma_\phi = 0{,}258\ MPa$ [1,8%], as shown in figure 30, shows that FRP composite pipe unconditioned small strain to the time dependent prediction but when at time dependent 40000 minutes the WI specimen, P8W453PBT of FRP composite pipes properties over crossed the unconditioned specimen, P5V453PBT of FRP composite pipes. As shown in the figure 30, the viscoelastic strain of unconditioned specimen, P5V453PBT decreases small deformation under strain lifetime time prediction and the viscoelastic strain of WI specimen P8W453PBT remains small under strain lifetime time prediction. The viscoelastic strain of DI specimen, P13D453PBT, didn't show extrema deformation at strain lifetime time prediction. Meanwhile the SWI specimen, P10SWI453PBT, the viscoelastic strain at failure continue decreasing extremely.

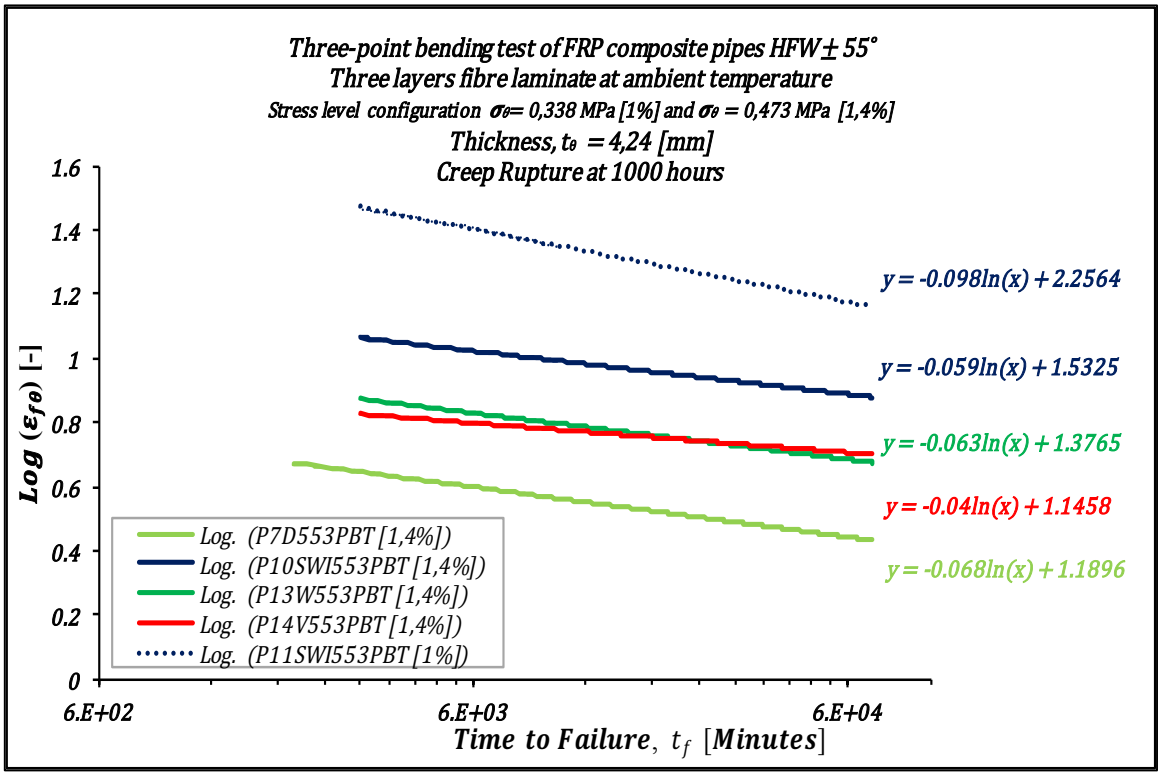

Figure 31. Failure lifetime prediction of FRP composite pipes HFW $\pm 55°$ at 1000 hours

The HFW $\pm 55°$ at 1000 hours' failure lifetime is shown in figure 31, under two different stress level configurations $\sigma_\theta = 0{,}338\ MPa$ [1%] and $\sigma_\theta = 0{,}473\ MPa$ [1,4%]. The FRP composite pipe in SWI specimen, P11SWI553PBT, at stress level configuration $\sigma_\theta = 0{,}338\ MPa$ [1%] perform the small strain occurred during 1000 hours' prediction in comparison with the FRP composite pipes SWI specimen, P10SWI553PBT at stress level configuration $\sigma_\theta = 0{,}473\ MPa$ [1,4%] which is extremely high.

Meanwhile, HFW ±55° FRP composite pipe at stress level $\sigma_\theta = 0{,}473\ MPa$ [1,4%], SWI specimen, P10SWI553PBT in comparison with the WI specimen, P13W553PBT and unconditioned specimen, P14V553PBT, viscoelastic strain is still adequate consideration or and DI specimen, P7D553PBT extremely low where the strain failure lifetime prediction decrease rapidly. The unconditioned specimen, P14V553PBT and WI specimen, P13W553PBT of FRP composite pipes have approximately the same viscoelastic strain at 1000 hour where the strain failure lifetime prediction remaining constant until the maximum failure time. But the WI specimen, P13W553PBT of FRP composite pipes as figured out in the graph the failure viscoelastic deformation outride the unconditioned specimens, P14V553PBT therefore, under the 1000 hours' regression analysis the WI specimen, P13W553PBT FRP composite pipes strain reach 0,4 at failure time.

Strain of FRP composite pipe vs Failure time data regression analysis for HFW ±55° performed as;

Unconditioned specimen, P14V553PBT [1,4%] logarithmic regression analysis model

$$1000\text{h}\log(\varepsilon_f) = 1{,}1458 - 0{,}041\log(t_u)$$

Seawater immerse specimen, P11SWI3PBT logarithmic regression analysis model at stress level 1%

$$1000\text{h}\log(\varepsilon_f) = 2{,}2564 - 0{,}098\log(t_u)$$

Seawater immerse specimen, P10SWI553PBT logarithmic regression analysis model at stress level 1,4%

$$1000\text{h}\log(\varepsilon_f) = 1{,}5325 - 0{,}059\log(t_u)$$

Water immerse specimen, P13WI553PBT [1,4%] logarithmic regression analysis model

$$1000\text{h}\log(\varepsilon_f) = 1{,}3765 - 0{,}063\log(t_u)$$

Diesel immerse specimen, P7D553PBT [1,4%] logarithmic regression analysis model

$$1000\text{h}\log(\varepsilon_f) = 1{,}1896 - 0{,}068\log(t_u)$$

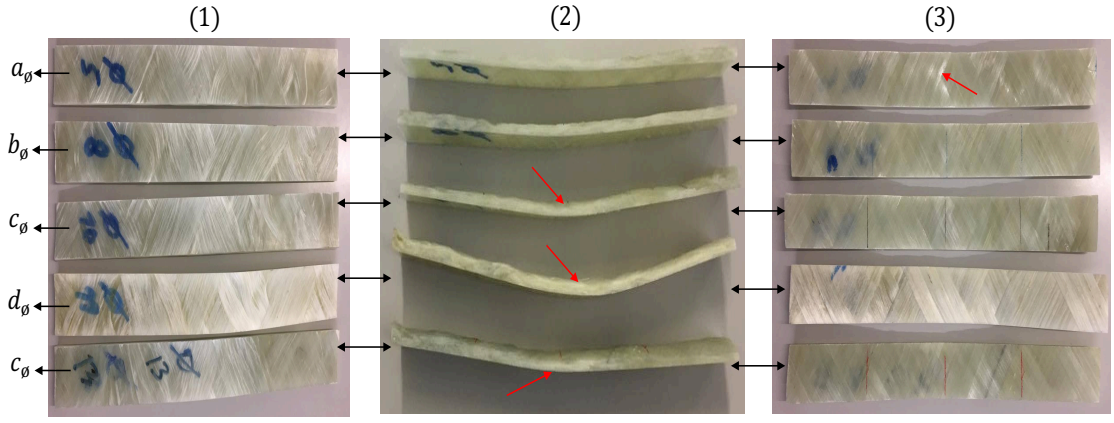

a_ϕ. P5V453PBT b_ϕ. P8W453PBT c_ϕ. P10SWI453PBT d_ϕ. P11W453PBT-T60 e_ϕ. P13D453PBT

Figure 32. Three-point bending creep test types of FRP composite pipes HFW ±45°, $\boldsymbol{d_y} \leq$ 24 mm

Failure deflection of three-point bending creep test by visual analysis of FRP composite pipe HFW ±45° and HFW ±55° are shown in the figure 32 and figure 33. For the HFW

±45° of FRP composite pipe unconditioned specimen P5V453PBT, WI specimen P8W453PBT, SWI specimen P10SWI453PBT and DI specimen, P13D453PBT occurred whitening color at deflection zone from the bottom of the circular arc specimen of FRP composite pipe as shown in the figure 32 part (1) [28-34].

For the WI specimen, P11W453PBT-T60 at 60°C occurred orange lighter color 80%. The failure crack deflection randomly appears whitening color at anvil contact of deep deflection as shown in figure 32 part (2) and all FRP composite pipe specimens occurred visually unrecovered deflection. For the specimen P11W453PBT-T60 at 60°C occurred high deflection unrecovered from creep failure deflection. In figure 32 part (3) specimen P5V453PBT occurred small gray -50% but specimens P8W453PBT, P10SWI453PBT, P11W453PBT-T60 and P13D453PBT are not occurred any changed colors.

Failure deflection types of HFW ±55 of FRP composite pipe shown in the figure 33-part (1) bottom zone shown that for the SWI specimen, P4SWI553PBT and DI specimen, P7D553PBT occurred whitening darker 15% colors from three-point bending loading with stress level 1,8% for SWI specimen P4SWI553PBT and three-point bending loading with stress level 1,4% for DI specimen P7D553PBT randomly appears whitening colors. In the specimens HFW ±55° WI at 60°C for specimen P9W553PBT-T60 occurred orange lighter color 80%. Failure deflection DI specimen P10D553PBT, SWI specimen P11SWI553PBT and WI specimen P13W553PBT from anvil loading surface visually not occurred any change in color of surface but at the slip surface ran domly appears whitening crack propagation along the fibre direction.

For the unconditioned specimen, P14U553PBT, randomly appear dark whitening color at anvil loading surface then at the slip side appears whitening of fibre and matrix crack along the fibre direction.

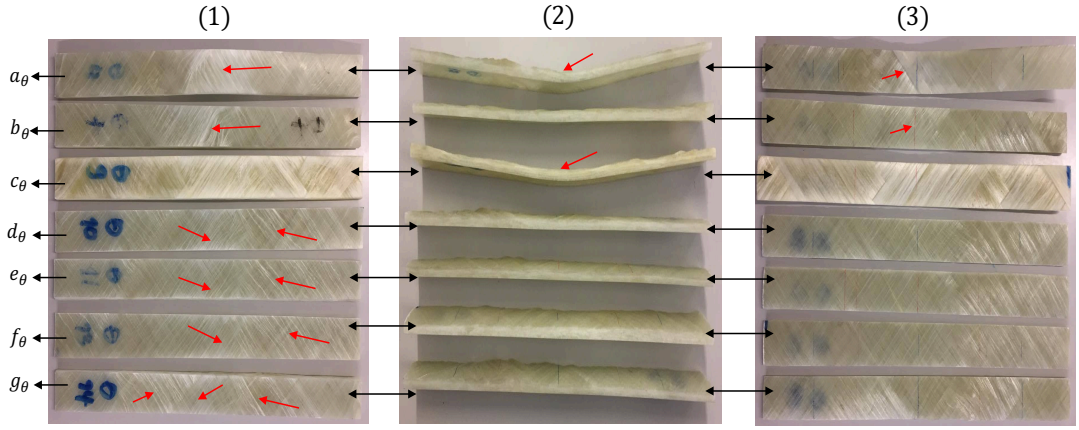

a_θ. P4SWI553PBT [1,8%] b_θ. P7D553PBT c_θ. P9W553PBT-T60 d_θ. P10SWI553PBT [1,4%] e_θ. P11SWI553PBT [1%] f_θ. P13W553PBT g_θ. P14V553PBT

Figure 33. Three-point bending creep test types of FRP composite pipes HFW ±55°, $\boldsymbol{d_y} \leq$ 24 mm

In the creep failure deflection of FRP composite pipe HFW ±55° as shown in the figure 33 part (2) occurred unrecovered creep deflection for SWI specimen P4SWI553PBT at stress level 1,8% and for WI specimen at 60°C P9W553PBT-T60 occurred outride unrecovered creep deflection. The HFW ±55° SWI specimen, P11SWI553PBT at stress level 1% and stress level 1,4% of SWI specimen P10SWI553PBT, DI specimen

P7D553PBT, WI specimen P13W553PBT and unconditioned specimen P14V553PBT visually occurred recoverable specimen of creep deflection from the constant loading.

For FRP composite pipe HFW $\pm 55°$, as shown in the figure 33 part (3), the anvil loading contact from upper surface of FRP composite pipe specimen for SWI specimen P4SWI553PBT at stress level 1,8% and DI specimen P7D553PBT at stress level 1,4% similarly occurred dark whitening color propagation at creep deflection. Meanwhile, the SWI specimen P10SWI553PBT, WI specimen P13W553PBT and unconditioned specimen P14V553PBT at stress level 1,4% and the SWI specimen P11SWI553PBT at stress level 1% did not occurred any color effect of fibre and matrix at the stress constant loading of three-point bending creep test.

4.2 References

1]. D1598-02, ASTM. (2002). Standard Test Method for Time-to-Failure of Plastic Pipe Under Constant Internal Pressure.

2]. D1599-99, ASTM. (2000). *Standard Test Method for Resistance to Short-time Hydraulic Pressure of Plastic Pipe, Tubing, and Fitting.* ASTM International.

3]. D2992-01, ASTM. (2001). *Standard Practice for Obtaining Hydrostatic or Pressure Design Basis for "Fiberglass" (Glass-Fiber-Reinforced Thermosetting-Resin) Pipe and Fitting.* ASTM International.

4]. D3517-04, ASTM. (2004). *Standard Specification for "Fiberglass" (Glass-Fiber-Reinforced Thermosetting-Resin) Pressure Pipe.* ASTM International.

5]. Hawa A, Abdul Majid M. S, Afendi M, Marzuki H. F. A, Amin N. A. M, Mat F. and Gibson A. G. (2016). "Burst strength and impact behaviour of hydrothermally aged glass fiber/epoxy composite pipes." Materials & Design 89: 455-464.

6]. Abdul Majid M. S, Afendi M, Afendi P, M. Haslan, Krishnan P, Amin A. M, (2014). Ageing effects on burst pressure test of impacted glass fibre reinforcement epoxy (GRE) pipes. *Trans Tech Publications, Switzerland, 695*, 717-720.

7]. Deniz M. E, Ozdemir O, Ozen M, and Karakuzu R. (2013). Failure pressure and impact response of glass'epoxy pipes exposed to seawater. *Elsevier, Ltd, 53*, 355-361.

8]. Gemi L, Tarakçioğlu N, Akdemir A. and Şahin Ö. S. (2009). "Progressive fatigue failure behavior of glass/epoxy ($\pm$75)" Filament-wound pipes under pure internal pressure." Materials & Design 30(10): 4293-4298.

9]. Kim H-Y, Y-H. Park, Y-J You and C-K. Moon (2008)."Short-term durability test for GFRP rods under various environmental conditions." Composite Structures 83(1):37-47.

10]. Gibson A. G, Ortheguy Torres M. E, Browne T.N.A, Feih S, and Mouritz A.P, (2010). High temperature and fire behaviour of continuous glass fibre/polypropylene laminates. *Composite: Part A, 41*, 1219-1231.

11]. Keller Michael W, Jellison B. D, Ellison T. (2013). Moisture effects on the thermal and creep performance of carbon fiber/epoxy composite for structural pipelines repair. *Elsevier Ltd*, 45, 1173-1180.

12]. Pavlov D. G, (2013) Composite Materials in Piping Application: Design, Analysis and Optimization of Subsea and Onshore Pipelines from FRP Composites. DEStech Publication, ISBN No. 978-1-60595-029-7

13]. Banakar P, Shivananda H. K, and Niranjan H. B. (2012). Influence of fiber orientation and thickness on tensile properties of laminated polymer composites. *International Journal of Pure and Applied Science and Technology, 9(1)*, 61-68.

14]. D3039/D3039M-00, ASTM. (2000). *Standard Test Method for Tensile Properties of Polymer Matrix Composite Materials.* ASTM International.

15]. D638-08, A. (2008). *Standard Test Method for Tensile Properties of Plastics.* ASTM International.

16]. Rafiee, R. (2016). "On the mechanical performance of glass-fiber-reinforced thermosetting-resin pipes: A review." Composite Structures 143: 151-164.

17]. Baker A, Dutton S, and Kelly D, (2004). *Composite Materials for Aircraft Structure* (Second Edition ed.). American Institute of Aeronautics and Astronautics, Inc.

18]. D790-02, ASTM. (2002). *Standard Test Method for Flexural Properties of Unreinforced and Reinforced Plastics Electrical Insulating Materials.* ASTM International.

19]. D2990-01, ASTM. (2001). *Standard Test Method for Tensile, Compressive, and Flexural Creep and Creep-Rupture of Plastics.* ASTM International.

20]. Hodgkinson, J. M. (2000). *Mechanical testing of advanced fibre composite.* Woodhead publishing limited Cambridge England.
21]. Hearn, E. J. (1997). *Mechanics of Materials 2* (Third Edition ed.). Butterworth Heinemann.
22]. Saidane, E. H., D. Scida, M. Assarar, H. Sabhi and R. Ayad (2016). "Hybridization effect on diffusion kinetic and tensile mechanical behaviour of epoxy based flax–glass composites." Composites Part A: Applied Science and Manufacturing 87: 153-160.
23]. Martin R, (The Institute of Materials, Minerals & Mining, 2008) The Aging of Composites, Woodhead Publishing and Maney Publishing
24]. Faria H, Guedes R. M. (2010). Long-term behaviour of GFRP pipes: Reducing the prediction test duration. *Elsevier Ltd*, 29 (2010) 337-345.
25]. Guedes R. M, Sá A. (2010). On the prediction of long-term creep-failure of GRP pipes in aqueous environment. *Polymer Composites, Elsevier Ltd, 31*, 1047-1055.
26]. Na L, Sirong Z, Jianzhong C, Xi F. (2015). Long-term behavior of GFRP pipes: Optimizing the distribution of failure points during testing. *Elsevier Ltd*, 48, 7-11.
27]. Birur, A. (2008). *Time-dependent damage evolution in multidirectional polymer composite laminates.* The University of Manitoba, Department of Mechanical and Manufacturing Engineering. Master Thesis.
28]. T. Shaw Montgomery, MacKnight W. J. (2005). *Introduction to polymer viscoelasticity.* Wiley Interscience.
29]. Enamul Hossain, M. (2011). "The current and future trends of composite materials: an experimental study." Journal of Composite Materials 45(20): 2133-2144.
30]. Greentech, G.(2016) "FRP Pressure Pipe". Retrieved from www.gilgwang.co.kr.
31]. Langhelle, M. B. (2011). *Pipelines for Development at Deep Water Fields.* University of Stavanger, Faculty of Science and Technology. Offshore Technology/ Marine and Subsea Technology, Master Thesis.
32]. Marsh, G. (2009). Composite pipe capture water and sewage markets. *Reinforced Plastics*, 53, 18-21.
33]. Davies P, Boisseau A, Choqueuse D, Peters L, Renaud C, Nickel R, Thiebaud F, Perreux D. (2010). Marine Composite for Ocean energy Application: Ensuring long-term durability. *Third International Conference on Ocean Energy.*
34]. Roylance, D. (2008). *Mechanical Properties of Materials* . MIT Publisher.

5. Conclusions

5.1 Burst Pressure Test of FRP Composite Pipes

Burst pressure of FRP composite pipe was not possible to perform due to several disturbances in the experimental apparatus setup. There are several aspects that occurred; oval shape of FRP composite pipe from inner and outer diameter of FRP composite pipe, occurred crack propagation from fastening of FRP composite pipe and lid fastening to the circular arc steel are not good fix of HFW $\pm 45°$ and HFW $\pm 55°$.

5.2 Tensile Test of FRP Composite Pipes

Fibre and matrix ageing of HFW $\pm 45°$ and HFW $\pm 55°$ diesel immersion specimen, P7D45TT and diesel immersion, P3D55TT of FRP composite pipes at ambient temperature consider as high maximum tensile stress, where the maximum tensile stress approach to 17,048 MPa and 37,307 MPa. This property is considered as appraisable for external effects of handling pipelines for offshore and onshore pipelines, oil rig installation and chemical industry of FRP composite pipe. Sea water immersion specimens, P6SWI45TT of HFW $\pm 45°$ and P8SWI55TT of HFW $\pm 55°$ also perform adequate results for offshore and onshore pipeline production and subsea pipeline installation.

The rupture type of HFW $\pm 45°$ of FRP composite pipes is short cross propagation at fibre and matrix surface and rupture type of HFW $\pm 55°$ of FRP composite pipes is long cross break propagation and along fibre direction. Therefore, the fibre rupture is whitening and peeling then pull out at the surface of FRP composite pipes.

5.3 Three-Point Bending Creep Test of FRP Composite Pipes

Ageing condition of HFW $\pm 45°$ of FRP composite pipes in three-point bending unconditioned specimen, P5V453PBT and water immersion specimen P8W453PBT induced small strain for sewage system application that occurred for 10080 minutes at ambient temperature and constant loading $\sigma_\theta = 0{,}258$ MPa [1,8%].

FRP HFW $\pm 55°$ composite pipe from sea water ageing condition at different stress level configurations 1%, 1,4% and 1,8% loading condition perform the viscoelastic time dependency at stress level configuration 1% of seawater immerse, P11SWI553PBT specimen is required adequate result for offshore industry applications. Stress level configuration at 1,4% of FRP composite pipe figure out that with HFW $\pm 55°$ for sea water immersion P10SWI553PBT, the viscoelastic properties at 10080 minutes is recommendable for FRP composite pipe in offshore and onshore pipelines applications.

Creep compliance of FRP composite pipe HFW $\pm 45°$ specimens P5V453PBTT and P8W453PBT at stress level configuration 1,8% at 10080 minutes, the lifetime properties are still adequate at lower creep compliance level in comparison with FRP composite specimen P13D453PBT and SWI specimen P10SWI453PBT. Meanwhile, the FRP $\pm 55°$ composite specimen lifetime viscoelastic considers SWI [1%] specimen, P11SWI553PBT and SWI [1,4%] specimen, P10SWI553PBT perform higher lifetime viscoelastic at 10080 minutes. The

unconditioned specimen, P14V553PBT and WI specimen, P13W553PBT [1,4%] also perform adequate lifetime viscoelastic under 10080 minutes.

The failure lifetime analysis of FRP composite pipe from different ageing conditions at 1000 hours' prediction of HFW $\pm 45°$ and HFW $\pm 55°$ shows that the viscoelastic lifetime degradation for HFW $\pm 45°$ unconditioned, P5V453PBT [1,8%] and water immersion, P8W453PBT [1,8%] viscoelastic degradation extreme small in compare to the diesel immersion, P13D453PBT [1,8%] and water immersion, P8W453PBT [1,8%] whereas the viscoelastic degradation is extreme large.

Meanwhile the HFW $\pm 55°$, the failure lifetime degradation of different ageing conditions shows that the viscoelastic degradation at different stresses levels of sea water immersions, P11SWI553PBT [1%] and P10SWI553PBT [1,8%] exist small viscoelastic degradation in compare to the water immersion, P13W553PBT [1,4%] and unconditioned, P14V553PBT [1,4%] extreme decrease at viscoelastic degradation.

6. Future Work

Burst pressure experimental data acquisition was not approachable, as many affected by many disturbances in experimental apparatus setup. Therefore, further work for this thesis proposal is burst pressure of FRP composite pipe HFW $\pm 45°$ and HFW $\pm 55°$ in different ageing condition as unconditioned, water immersion, sea water immersion and diesel immersion. The immersion time and testing time of burst pressure of FRP composite pipe could be immerse similar as three-point bending creep test for period of short-time.